GRADO EN INGENIERIA INDUSTRIAL

TRABAJO FIN DE GRADO

PREPROCESSING OF EMG SIGNALS

Autor: Álvaro Martín Martín
Director: Romano Giannetti

Madrid
Junio, 2023

Declaro, bajo mi responsabilidad, que el Proyecto presentado con el título

……..……**PREPROCESSING OF EMG SIGNALS**……..…

……

en la ETS de Ingeniería - ICAI de la Universidad Pontificia Comillas en el curso académico …**2022/23**... es de mi autoría, original e inédito y no ha sido presentado con anterioridad a otros efectos. El Proyecto no es plagio de otro, ni total ni parcialmente y la información que ha sido tomada de otros documentos está debidamente referenciada.

Fdo.: **ÁLVARO MARTÍN MARTÍN** Fecha: **23/06/2023**

Autorizada la entrega del proyecto

EL DIRECTOR DEL PROYECTO

Fdo.: **ROMANO GIANNETI** Fecha: **23/06/2023**

Resumen

Una electromiografía (también conocida como EMG) es la representación de la señal eléctrica producida por la actividad muscular. Para poder medir estos impulsos se utilizan electrodos. Estos electrodos pueden ser de varios tipos, pero los más comunes son los electrodos de superficie (normalmente los adhesivos desechables) y los electrodos de aguja. Estos últimos se insertan dentro del músculo de interés para registrar el EMG utilizando de la aguja mientras que el otro simplemente se coloca sobre la piel.

Cada tipo de electrodo tiene sus ventajas e inconvenientes. Los electrodos de aguja proporcionan lecturas precisas y de un área muy concreta, mientras que los electrodos de superficie son fáciles de instalar y tienen poco riesgo de infección al usarlos. Dependiendo de la aplicación, el tipo de electrodo será distinto, e incluso para algunas aplicaciones puede ser necesario construir un electrodo personalizado para adaptarse a las necesidades específicas del caso. En el caso particular del proyecto, se utilizarán electrodos de superficie desechables para medir las EMG, ya que son los más seguros y relativamente económicos.

Con el fin de procesar la señal EMG, se diseña un circuito de preprocesamiento analógico electrónico. Este circuito consta de cuatro etapas principales: ganancia, filtrado, rectificación y una envolvente. Las señales EMG tienen un voltaje muy bajo (alrededor de 1 mV de amplitud). Por lo tanto, la etapa de ganancia consta de un amplificador de precisión que dará la ganancia necesaria para aumentar el voltaje de la señal. La etapa de filtrado ayuda a reducir cualquier ruido no deseado de diferentes fuentes de ruido (consulte el Capítulo 2 para obtener más información). El filtro principal será un filtro de Butterworth de cuarto orden con una frecuencia de corte de 10 kHz. La rectificación se realizará utilizando un rectificador de precisión para distorsionar la señal lo menos posible. El detector de envolvente tendrá una constante de tiempo de 0,3 s, derivada del estudio realizado sobre la Figura 3.18.

Una vez finalizado el preprocesamiento analógico de la señal EMG, se necesita digitalizar la señal. Para ello, se debe seleccionar un tiempo de muestreo adecuado y, siguiendo los resultados de la Figura 5.9, un tiempo de muestreo de alrededor de 20 ms será adecuado para los requerimientos de este proyecto. Usando este tiempo de muestreo (y como se muestra en la Ecuación 6.2), la cantidad de datos es reducida considerablemente, facilitando su procesado (hasta los 400 bits/s). Con toda esta información, la señal puede ser transmitida a un sistema digital donde será procesada para el control de otros sistemas.

Abstract

Electromyographies (or EMG) are electrical recordings of muscle activity. In order to record these impulses, electrodes are used. These sensors can be of many types, but the most commonly used forms are surface electrodes (such as disposable foam-pad electrodes) and needle type electrodes. The latter of these is inserted inside the muscle of interest in order to record the EMG with help from the needle, while the other one simply rests on top of the skin.

Each type of electrode has its limitations and advantages, needle electrodes give precise and short-area readings, while surface electrodes are easy to install and have little risk of infection when using them. Depending on the application, the type of electrode will vary, for some applications it might even be required to build a custom electrode to suit the specific needs of the measurement. In the particular case of the project, foam-pad electrodes will be used to measure all EMGs since they are the safest and relatively cheap.

In order to process the EMG signal, an electronic analog preprocessing circuit is designed. This circuit has four main stages: gain, filtering, rectifier and envelope detector. EMG signals have a very low voltage (around 1 mV amplitude). Therefore, the gain stage consists of a precision amplifier which will give the necessary gain to boost the voltage of the signal. The filtering stage helps to reduce any unwanted noise from different noise sources (see Chapter 2 for more information). The main filter will be a fourth order Butterworth Filter with a cut frequency of 10 kHz. The rectifier will be a precision rectifier in order to distort the signal as little as possible. The envelope detector, will have a time constant of 0,3 s as studied in Figure 3.18.

Once the analog preprocessing of the EMG signal is finished, it is the turn of the digitalisation of the signal. In order to do this, an adequate sampling time must be selected and following the results on Figure 5.9, a sampling time of around 20 ms will be suitable for the needs of this project. Using this sampling time, as shown on Equation 6.2, the data transfer can be reduced to a viable point (400 bits/s). With this data, all of the relevant information of the signal is transmitted from the measuring device onto the digital system where it will be processed in order to control other systems.

GRADO EN INGENIERIA INDUSTRIAL

TRABAJO FIN DE GRADO

PREPROCESSING OF EMG SIGNALS

Autor: Álvaro Martín Martín
Director: Romano Giannetti

Madrid
Junio, 2023

Contents

1 Introduction

Engineering and medicine today are more intertwined than ever before. The constant advancements made by engineers have lead to great improvements in every-day life, industry and many other fields. The most relevant field for this paper is undoubtedly medicine. Medical instrumentation devices have evolved at an outstanding rate. Being assisted by a robot in complex operations is more common as time passes; new materials are being developed to create prosthetic limbs; and technologies like 3D printing are making their way into this world.

The main goal of engineering is to find the best solution to a complex problem. This takes into account many relevant aspects: economic, simplicity of design, viability, mass-production if necessary and usually implies having a great scalability (low marginal costs).

With the help of medicine, engineers can develop solutions to aid doctors in healing or regaining lost faculties. An example of this could be a person who has lost mobility in a limb due to an accident where their nerve severed. This damage is, in most cases, irreversible. Nonetheless, engineers can develop solutions to partially regain some of the movement via a robotic prosthesis (for example). This solution would require a complex analysis of different body signals, as well as the development of software and hardware for the robotic prosthesis.

An electromyography (onwards referred to as an EMG) is an electrical recording of muscle activity. In brief, muscles contract or relax depending on the voltage and frequency at which pulses are emitted by the nerves connected to them. These different voltage and frequencies can be pre-processed with an analog circuit to later be interpreted by a micro-controller and control a prosthesis.

The main characteristics of an EMG signal are the amplitude and frequency of the signal. These characteristics will vary depending on the characteristics of the muscle (size, activity, etc. . .).

It is quite straightforward to deduce that, when no EMG signal is present, there will be no electrical stimulation of the muscle fibres and therefore no muscle force. It is

quite useful to represent the force-EMG[1] relationship in a graph. As mentioned before, it varies depending on the muscle targeted, but the main conclusion is that, strictly speaking, the behaviour is non-linear. In figure 1.1, this non-linearity can be seen. Large muscles such as the biceps take a curvilinear relationship, while mall muscles such as the first dorsal interosseous muscle (FDI), take a quasi-linear relationship. As a first simplified approach, EMG relationship to force can be considered linear without causing much of an error, however in more precise applications, taking this non-linearity into account must be further investigated.

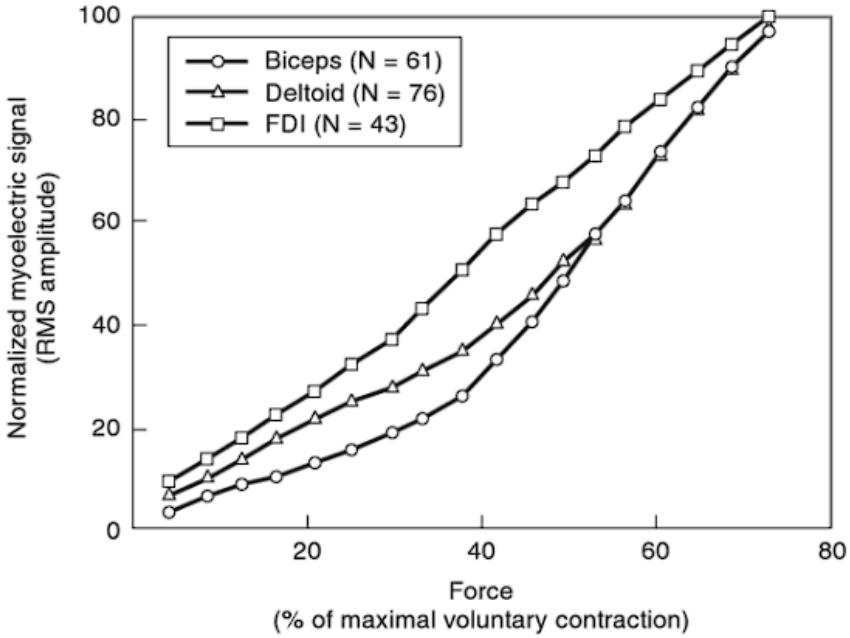

Figure 1.1. Representation of the emg-force relationship in different muscles (biceps, deltoid and FDI). N = number of average contractions of each muscle[1].

Frequency wise, the main spectrum of EMG signals is between the 20 to 300 Hz interval. Having a bandpass filter with cut frequencies in those mentioned before will represent most of the relevant data from an EMG singal.

1.1. EMG measurement

EMGs are recorded using electrodes. There are generally two types of electrodes: body-surface recording electrodes and internal electrodes. One of the most commonly used forms of body-surface recording biopotential electrodes is the metal-plate electrode. Essentially, it consists of a metallic conductor in contact with the skin (usually with a electrolyte[2] soaked pad). Different kind of pads have been developed for each specific need, the most relevant are the metal-disk electrodes. This kind can be used to measure an ECG[3]. They consist of a metal disk with a cable soldered to it, through which the signal is carried. They are mostly used for long-term measuring of signals and are

[1] RMS value
[2] an electrically conducting medium containing ions used to establish and maintain electrical contact
[3] electrocardiogram

fixed to the patient using surgical tape. For a shorter-term solution, there are similar devices known as disposable foam-pad electrodes (Figure 1.2). These work in the exact same way as the previous mentioned with the exception of being ready to apply to the patient out of the box and will just be thrown away when finished (minimizing the time dedicated to their maintenance). This kind of sensor does not have a cable soldered to them, but a connector, which allows for a quick connection and disconnection from the measuring system. The cost of these sensors is very low, making them ideal for many tests.

As expected, surface electrodes have a great disadvantage. Measuring a Single Motor Unit (SMU) is extremely complicated as these sensors can't be pointed directly at what we want to record. Having a metal disk (even the small ones) which covers an area in the skin means that the output signal is composed of many superimposed signals from other muscle groups (specially during powerful contractions).

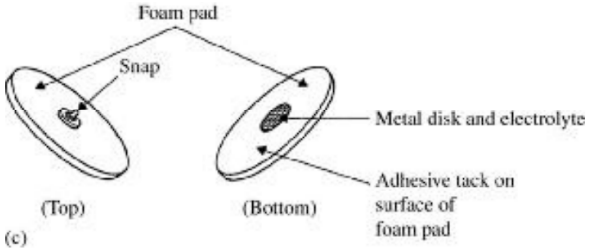

Figure 1.2. Disposable foam-pad electrodes [2].

Surface electrodes are placed on top of skin, which needs to be cleaned to guarantee proper contact (eliminating grease and dirt). In addition to this, the epidermis and subcutaneous layers have a capacitance and impedance, which complicate the correct measuring of signals. An equivalent circuit can be seen on Figure 1.3, where the different layers are modelled as capacitances and resistors. The values of said components vary according to the frequency[4][2].

Internal electrodes can also be used to measure biopotentials. They take the form of *percutaneous electrodes*, and what is most interesting about this kind is that they can be entirely internal. For example, a connection to a radio-telemetry transmitter, which transmits data to the outside of the body. This kind of sensors have some differences with surface electrodes: they do not need electrolyte gel; they do not have to contend with the electrolyte-skin interface (as it crosses the skin). It is frequent for an investigator to design his or her own electrode for their specific purpose, this leads to an enormous variety of types. The most common (Figure 1.4) are the insulated needle electrode, where the shank of the needle is insulated[5] leaving only the tip exposed. This kind of electrodes record the EMGs of a single muscle group acutely and can be removed if necessary. This makes their use in EMG recording extremely common.

[4]Skin impedance is approximately 200 kΩ at 1 Hz and 200 Ω at 1 MHz
[5]usually with an insulating varnish.

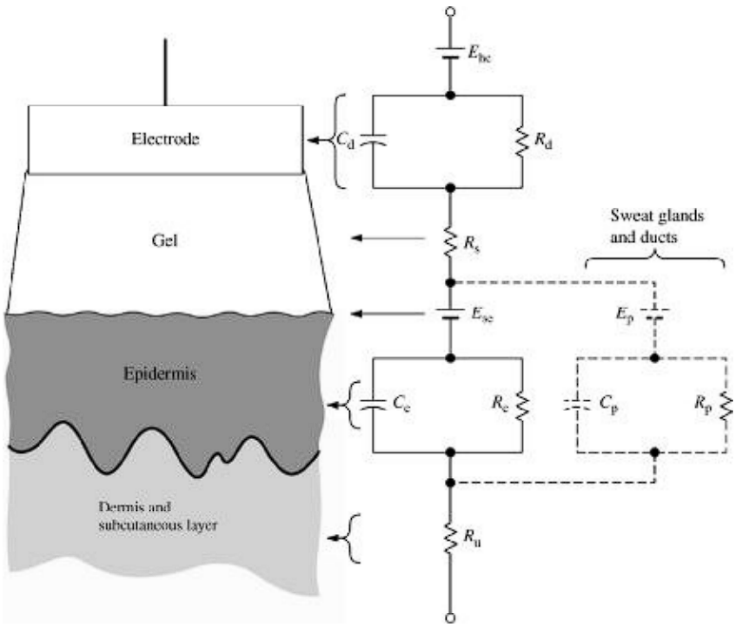

Figure 1.3. Equivalent circuit of a body-surface electrode placed against the skin [2] .

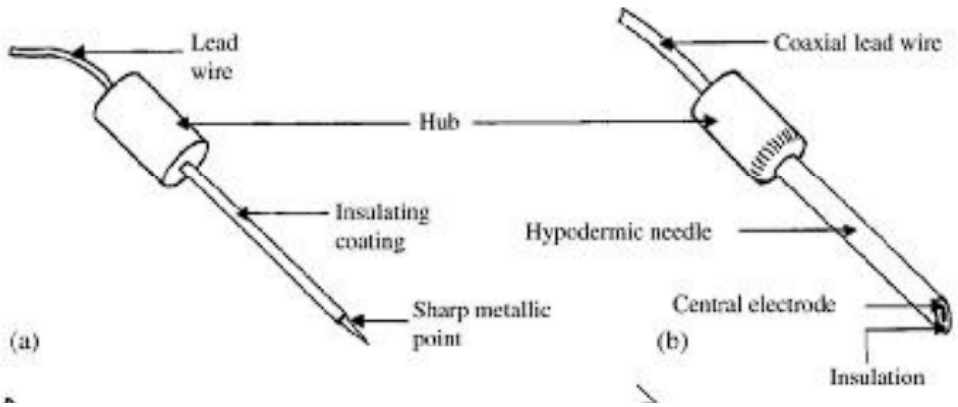

Figure 1.4. Insulated needle electrode (left) and coaxial needle electrode (left) [2].

1.2. Existing EMG processing hardware

The primary function of an EMG system is to faithfully record and process EMG signals for further analysis. These systems must have an adequate 'signal to noise' ratio. This can be achieved using analog and digital signal processing techniques.

1.2.1. Hospital EMG machines

In hospitals, EMG signals are used to detect or test for nerve and muscle disorders. Some of the symptoms may include[3]:

- Muscle disorders such as muscular dystrophy or polymyositis
- Diseases affecting the connection between muscle and nerve (myasthenia gravis, for example)
- Disorders of nerves outside the spinal cord (carpal tunnel syndrome, for example)

- Disorders that affect the motor neurons in the brain or spinal cord (ALS[6] or polio, for example)
- Disorders that affect the nerve root (herniated disk in the spine, for example)

An example of an EMG machine in a hospital can be the Neuropack X1 by Nihon Kohden, seen in figure 1.5. This EMG machine is used in the *Hospital Universitario de Getafe*, in Madrid.

EMG hospital machines make a peculiar ticking noise according to the parameters of the measured signal. The higher the frequency of the signal, the higher the frequency of the clicking. Also, the bigger the amplitude, the louder the clicking is. This audio is just an aid for doctors, it facilitates the diagnosis but does not give more information since it is extracted from the EMG signal measured.

Figure 1.5. Image of the Neuropack X1 measurement system used to process EMG signals amongst other types of body signals[4]..

The images in Figure 1.6 represent the EMG produced by the *Abductor Pollicis Brevis* muscle (otherwise known as the Thumb Abductor). The first image shows the placement of the surface electrodes (there are three electrodes, two in the image and a third inside an armband placed on the middle of the forearm acting as the reference point). The rest of the images are pictures of the screen of the Hospital EMG machine's screen showing small, medium and high activity in the muscle measured.

The general circuit schematic of a hospital EMG machine is represented on Figure 1.7. Here, $E0$ represents the reference electrode while $E1$ and $E2$ the measuriong electrodes. These signals are carried onto the electronics inside the system and output an analog signal and a sound queue. It has a control panel and other nuts and bolts. All the data is shown in a screen, where a with a mouse and keyboard, the GUI can be navigated.

[6]Amyotrophic Lateral Sclerosis

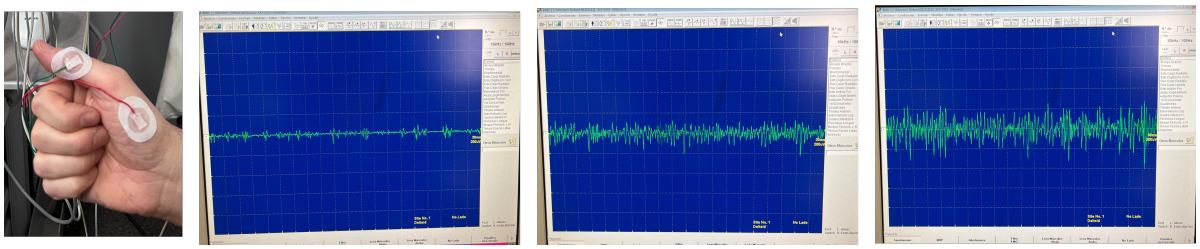

Figure 1.6. EMG signal examples measured with 1.5. Description of images: (1) electrode position, neutral is an armband attached to the forearm; (2) no muscle activity; (3) low muscle activity; (4) high muscle activity.

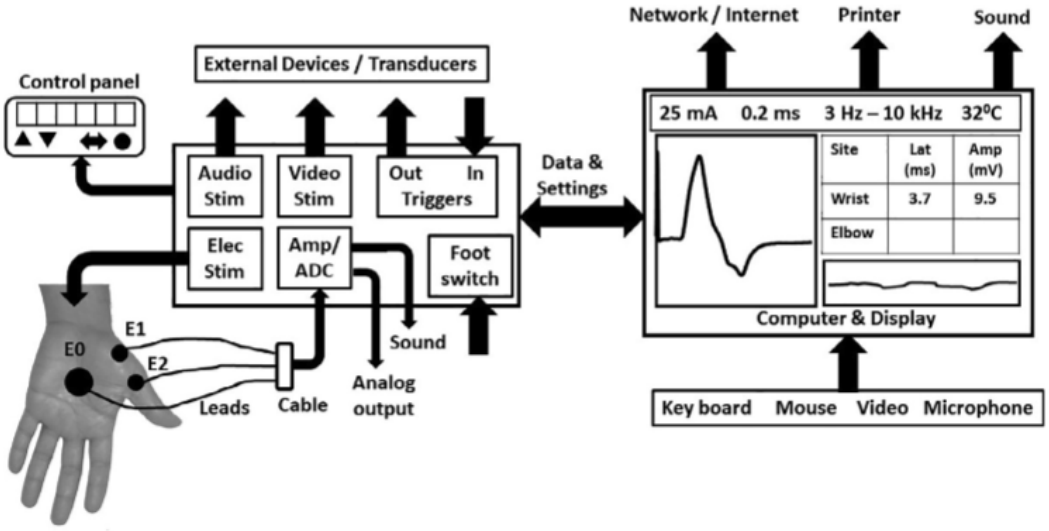

Figure 1.7. Schematic representation of a general EMG diagnosis system[5].

1.2.2. Arduino EMG processors

Due to EMGs being easy to measure, there are some consumer-grade solutions to an EMG machine. The circuit shown in Figure 1.8 works as shown in Figure 1.9, where the input signal (an EMG) is rectified[7] and then smoothed. The idea behind this circuit is for the output to be connected to a micro-controller (like an Arduino) and measure the output voltage of the circuit using one of the analog pins. This circuit is a great example of how an EMG might be processed, the only inconvenience is that much of the relevant data (such as number of peaks, frequency, peak voltage, etc...) is lost due mainly to the smoothing.

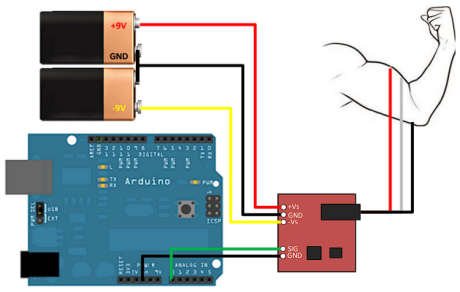

Figure 1.8. Muscle Sensor v3 [6].

[7]all signal values are turned positive

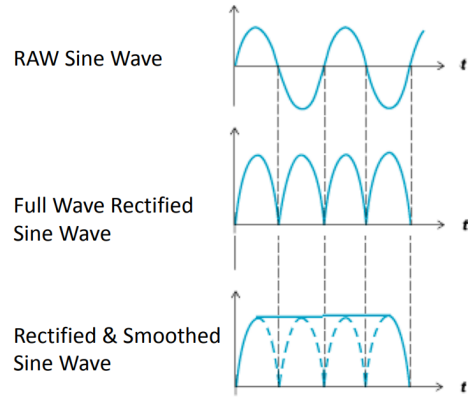

Figure 1.9. Muscle Sensor Operation [6].

There are current applications of EMG measurements to record muscle activity. Most of them use surface sensors to record said signal, which has the disadvantages mentioned before. These sensors can be hard to manage, specially when many of them are placed (see Figure 1.10). There are interferences, a chance for them to detach and cause a faulty measurement and generally mixing cables and living beings tends to be fidgety. People get tangled and it may be quite uncomfortable for the patient.

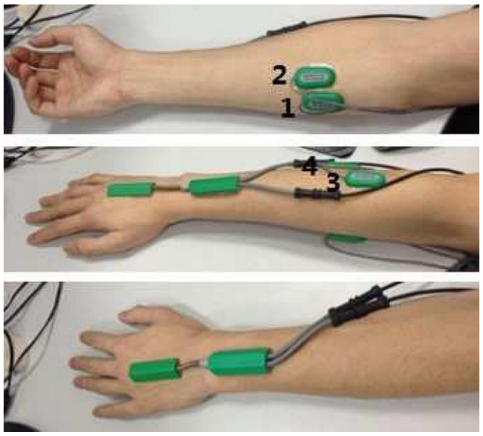

Figure 1.10. Surface EMG sensors example [6].

2

EMG Noise

EMG signal attributes depend on the subject. Characteristics like skin formation, blood flow velocity, body temperature, fat percentage and the surrounding environment can affect the measurement of an EMG. Each one of these attributes contributes to generating noise in the signal in a different way. The main challenges in eliminating each type of noise are explained in this section.

Noise usually implies a any random superimposed disturbance which corrupts the signal we desire to measure and increases uncertainty when taking decisions based on this signal. Due to the random nature of the disturbance, statistical mathematical methods are required in order to analyse it. Noise is inevitable outside of simulations, in controlled environments it can be reduced to a minimum, but in the day-to-day world it is a characteristic which needs to be dealt with. In figure 2.1, a comparison of how noise affects an ideal sine wave can be seen. The first image shows a small noise (10% of the sine wave amplitude), the second one shows a greater noise (50%) and the third shows an extreme case where the noise amplitude is equal to the signal amplitude. This last example can become plausible when measuring small voltages.

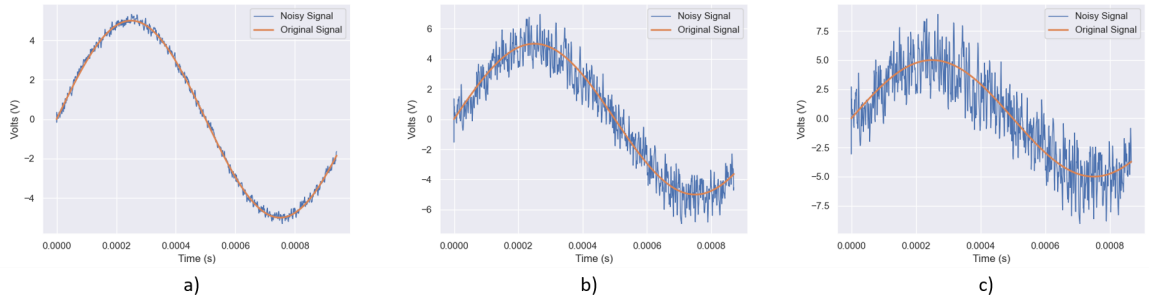

Figure 2.1. Comparison of signal to noise ratio in a sine wave (1 kHz). Figure a) shows a 10% SNR; figure b) a 50% SNR; and figure c) a 100% SNR.

Noise can be reduced by the use of filters. For example, if a low-pass filter is used on the previous signals, we get the results shown in 2.2. It is quite straight-forward to deduce that the lower the noise the better the signal is reconstructed. In the last image

we can see that even thought the signal is still quite deformed, it will be suitable for many applications.

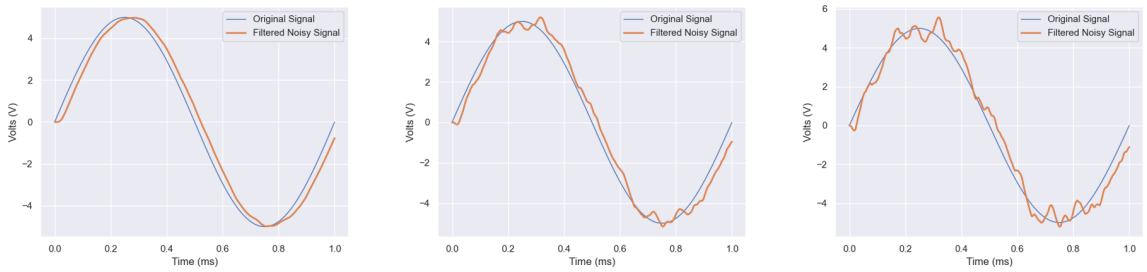

Figure 2.2. Comparison of filtered noise in a sine wave. Figure a) shows a filtered 10% SNR; figure b) a filtered 50% SNR; and figure c) a filtered 100% SNR.

2.1. Noise sources

2.1.1. Noise in the electrode

In most fields, the very action of trying to measure a value causes it to be modified. Electronics is no different. This noise receives the name of "inherent" due to the fact that it will be produced by the sensor itself and avoiding it is quite difficult. Noise frequency emitted in this category varies between 0 Hz and several thousand Hz. As explained in 1.1, surface electrodes are widely used. Electrodes made of silver/Silver chloride (10x1mm) grant a low signal-to-noise ratio and are electrically steady. As well as being affordable, this makes them a vastly used as surface electrodes [7]. High impedance electrodes reduce the quality of the signal but also reduce the signal-to-noise ratio. Therefore, depending on the application, both factors need to be taken into account when deciding which electrode to use.

2.1.2. Motion Artifacts

As explained in [8] motion artifacts produce the largest disturbances in an EMG, having a similar amplitude to that of the EMG. The dominant phenomenon that contributes to this noise generator is the movement of the electrode relative to the skin layers. When superficial electrodes are used, muscle movement under the skin must be taken into account. Different skin layers have different potentials, and shifting these layers leads to big interferences. However, the frequency range for these interferences is in the 0 to 10 Hz spectrum. It also must be taken into account that motion artifacts are non-stationary, time-varying electrical signals. This type of interference can be reduced by reducing the impedance of the skin. As shown by Tam and Webster [9], scratching the skin reduces these artifacts. As shown in Figure 2.3, abrasive tape (which produces a similar effect to scratching the skin) reduces significantly the impedance of the skin.

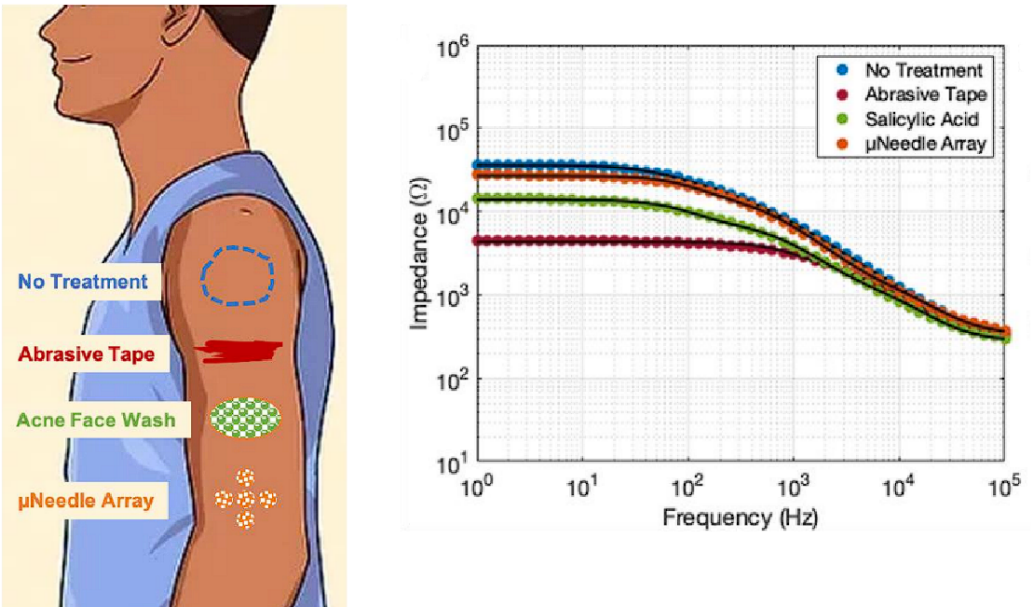

Figure 2.3. Variation of skin impedance with frequency and different skin treatments [10].

2.1.3. Electromagnetic interference

The human body is essentially an antenna. Our surface is constantly radiated with electrical and electromagnetic radiation. This radiation generates the electromagnetic noise. Since EMG signals are quite low-amplitude signals, electromagnetic noise can (under worst case conditions) be two to three times greater that the EMG signal itself. This can lead to huge mistakes when classifying these signals.

However, electromagnetic noise has a fundamental characteristic which can help us remove it. The main source of this noise is from the interference caused by electrical power lines (PLI). Hence, the dominant frequency of this noise is 50 Hz[1]. Therefore, a high-pass filter will be needed in order to remove these unwanted signals. The goal is to remove only this interference and not modify the EMG signal. If the PLI frequency is significantly lower than the EMG frequency, then the high-pass filter will work correctly. However, when analysing EMG frequencies that are closer to those of the PLI, information will be lost. Assuming a power line frequency of 50 Hz, the harmonics of the PLI are constructed by following equation 2.1:

$$PLI_{ref} = A_50cos(2\pi 50t) + A_100cos(2\pi 100t) + A_200cos(2\pi 200t) + A_300cos(2\pi 300t) + ... \quad (2.1)$$

Some of the solutions proposed for this problem by [11] include adaptive FIR notch filters, adaptive notch filters using Fourier transform and Laguerre filter. The general block diagram for most PLI cancelling system can be seen on 2.4.

[1] 60 Hz in some countries

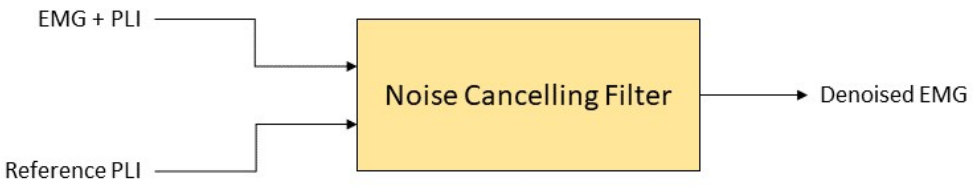

Figure 2.4. General PLI cancelling system block diagram.

2.1.4. Crosstalk

This section mainly applies to surface EMG signals. When an EMG signal form a non-monitored muscle group interferes with the desired EMG signal, this interfering EMG can be classified into Crosstalk noise. This noise can lead to a incorrect interpretation of the signal by the algorithm. As discussed on 1.1, crosstalk depends on many variables, such as: electrode size, placement, target muscle, inter-electrode distance and most importantly, the electrode type.

If a needle electrode was chosen, this interference would be greatly diminished, since these electrodes can accurately measure a muscle. However, if surface electrodes are used, this noise will be extremely difficult to filter. The amplitude of the noise will be of a similar amplitude (or lower) than the desired EMG signal. According to [12], this noise will be generated by the sum of three uncorrelated random variables. This is shown in equation 2.2, where the activity of the target muscle (Ti), the crosstalk from the remote muscle (Rb) and the crosstalk from other muscles (Ob) all add up to the recorded EMG activity (Tb).

$$T_b^2 = Rb_c^2 + T_i^2 + Ob_c^2 \tag{2.2}$$

Since this noise is random, the easiest solution to mitigate the effects is to carefully select the electrodes used, correctly prepare the surface of the skin (in the case of using surface electrodes) and take into consideration equation 2.2 when classifying the signals.

2.1.5. Internal Noise

Capacitive effects are often assumed negligible when analysing EMG data. EMG simulations are based (generally) on purely resistive models, where these effects do not exist. Muscle conductivity and permittivity are frequency-dependent[2]. According to Plonsey[13], the condition for neglecting capacitive effects in homogeneous bioelectromagnetic models is:

$$\frac{\omega \varepsilon_0 \varepsilon_r}{\sigma} \ll 1 \tag{2.3}$$

[2]This phenomenon is called dispersion

Where σ and ε_r, denote the conductivity and the relative permittivity of the tissue, and ω_o the angular frequency. $\varepsilon_0 = 8.85410^{-12}F/m$ is the permittivity of vacuum.

According to Stoykov et al.[14], these assumptions may not be valid for muscle tissue. Capacitive effects in EMG signals may vary from having a negligible influence to a considerable impact, depending on the combination of electric conductivity and permittivity used.

Conductivity is the material's capability to conduct electricity. It is a measurement of the current density (current per unit area) and the electric field strength in that area. The higher the conductivity, the easier it is for electricity to get across a material [15].

Permittivity (or dielectric constant) represents the ability of a material to store an electrical charge. It is the ratio of the electric flux per unit area to the electric field strength. The higher the electric permittivity, the easier it is for a material to store electric charge [15].

Hemingway et al. demonstrated that EMG signal activity is directly dependent on the amount of tissue between the electrode and the target muscle [16]. This is one of the reason why in 1.1 surface electrodes will have difficulty on recording EMG signals from deeper muscles. Their signal will be weaker, on top of possible cross-talk from other motor units.

2.2. Noise removal techniques

1. Filtering:
   Filtering is a widely used method to remove noise from signals. Filters can be implemented digitally or analogically and their main purpose is to remove the unwanted components from certain frequencies from the signal while keeping the rest intact. There are different type of filters, but the most commonly used in EMG processing are:

   a) Low Pass Filters: These filters allow frequencies below a cutoff frequency to pass while attenuating higher frequencies.

   b) Notch Filters: These filters attenuate a narrow band of frequencies, typically centered around the power line frequency (50 or 60 Hz), which is a common source of noise in EMG signals (as mentioned in Section 2.1.3).

2. Common Mode Rejection:
   This technique exploits the fact that noise often affects the possitive and negative terminals of an electrode in the same way. By amplifying a differential signal, noise can be significantly reduced. This is the reason why the surface electrodes used when measuring come in threes and not in pairs (one is the reference, and the other two are for the muscle of interest). Instrumentation amplifiers and differential amplifiers are commonly used to implement common mode rejection.

3. Wavelet Denoising:
   Wavelet de-noising is a technique that uses the properties of wavelet transforms to remove noise from EMG signals. The wavelet transform allows the decomposition of a signal into different frequency sub-bands. This technique has the inconvenient of only being possible to apply it digitally.

4. Independent Component Analysis (ICA):
   ICA is a statistical technique which separates a multivariable signal into its components. In EMG signal processing, ICA can be used to separate the desired EMG signals from other sources of noise or interference. By assuming that the sources are statistically independent, ICA can estimate the mixing matrix and recover the underlying EMG signals. This method is useful when dealing with EMG signals contaminated by motion artifacts (Section 2.1.2).

3

Electronics

As mentioned before in different chapters, the EMG signal will be measured using an electrode. After measuring this signal, due to its low voltage, an analog pre-processing circuit must be designed and implemented for the signal to be useful. Figure 3.1 represents a general block diagram of a possible solution to process this information into an easier to analyse wave.

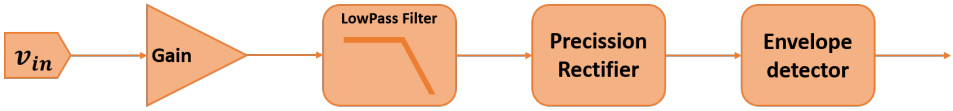

Figure 3.1. General block diagram of the different electronic analog preprocessing stages to process the input EMG signal..

The goal of the electronic design is to reduce as much as possible the amount of data processed by the measuring micro-controller. Therefore, the sample frequency must be the lowest possible. There are also some other constraints to this design: Power consumption must be reduced to a minimum, since in the final application this device will be running from a battery; supply voltage must be between $-5\,\mathrm{V}$ and $+5\,\mathrm{V}$.

3.1. Input Signal

Before measuring in the lab and in order to know what to expect, an EMG dataset will be used. After thorough research, a dataset from UCI's Machine Learning Repository[17] has been chosen. The device used to record EMG is a MYO Thalmic bracelet worn on the forearm. An image of the bracelet can be seen on Figure 3.2, it has eight identical sensors equally spaced through the forearm and in direct contact to the skin. These sensors record the data and transmit it via Bluetooth to the PC where the dataset is stored. In total, the dataset includes data from 36 subjects which performed a series of static hand gestures. Each gesture was performed two times. The gestures were performed for 3 seconds with a 3 second rest period in between gestures.

Since the dataset has a lot of information, a small portion of this information will be used for the initial design and later compared to other data. The chosen input will be

Figure 3.2. MYO Thalamic bracelet in forearm[18]..

seconds 27 to 33 of the first subject (the full input can be seen on Figure 3.3). The six second time interval mentioned before (Figure 3.4) corresponds to wrist extensions. This interval was selected due to it being one of the highest activity regions in the EMG signal. This signal has roughly a $2\,\mathrm{mV_{PP}}$[1] amplitude and is sampled at a frequency of $f_{s_{input}} = 1\,\mathrm{kHz}$ (1 ms time intervals).

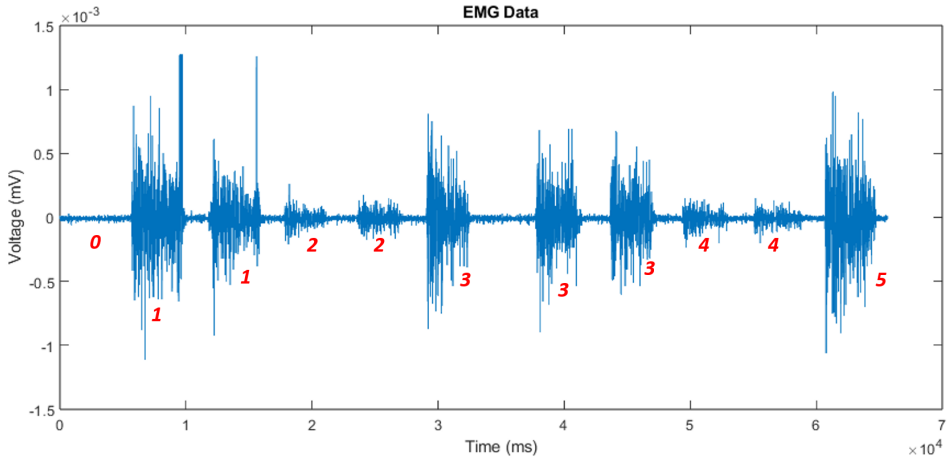

Figure 3.3. Full EMG recording in instance 01 of subject 01 in the dataset mentioned above[17]. 0 - hand at rest; 1 - hand clenched in a fist; 2 - wrist flexion; 3 - wrist extension; 4 - radial deviations; 5 - ulnar deviations.

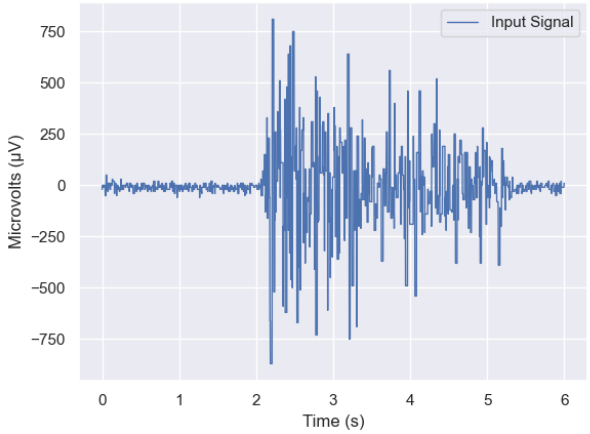

Figure 3.4. Input selection of EMG signal[17].

[1] Peak to peak voltage

3.2. Gain circuit

Due to the low amplitude of the input signal, a high gain stage is needed. Many other factors need to be taken into account, it must be a precise amplifier and have a low power consumption to meet the design criteria.

The AD8422[19] is a High Performance, Low Power, Rail-to-Rail Precision Instrumentation Amplifier which meets the requirements of this design.

The transfer function of the AD8422 is:

$$V_{out} = G \times (V_{IN}^{-} - V_{IN}^{+}) + V_{ref} \tag{3.1}$$

where:

$$G = 1 + \frac{19{,}8\,\mathrm{k\Omega}}{R_G} \tag{3.2}$$

The nearest 1% resistor values for common gains of 3.2 are shown on Table 3.1:

1% Standard Values of $R_G(\Omega)$	Calculated Gain
19,6 kΩ	2,010 V/V
4,99 kΩ	4,968 V/V
2,21 kΩ	9,959 V/V
1,05 kΩ	19,86 V/V
402 Ω	50,25 V/V
200 Ω	100,0 V/V
100 Ω	199,0 V/V
39,2 Ω	506,1 V/V
20 Ω	991,0 V/V

Table 3.1. Gains using 1% resistors

Using the input signal from Figure 3.4, the output of the gain stage using a gain of $1000\,\mathrm{V/V}$ ($R_G = 19{,}1\,\Omega$) is shown in Figure 3.7. The final signal will be of around 2 V and due to the amplifier being a precision one, it will have a low offset compared to the input signal.

Taking into account the data provided by the datasheet[19], and that yielded by the simulations ran from LTSpice, the current consumption of the amplifier is around 300 μA at $\pm$5 V.

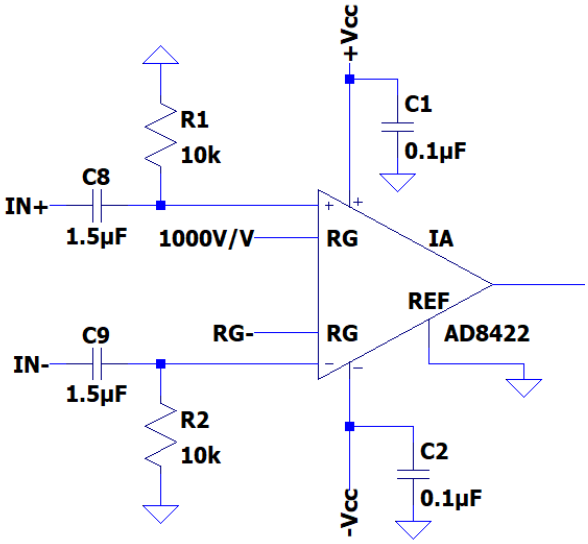

Figure 3.5. AD8422 connection schematic..

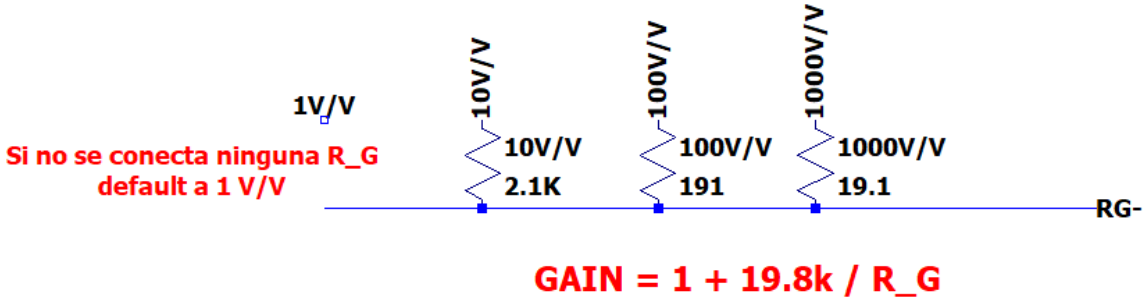

Figure 3.6. Manual variable R_G in order to simulate in LTSpice with ease different gains. Changing the R_G+ value between 1 - 10 - 100 - 1000 in 3.5, will change the gain to that value.

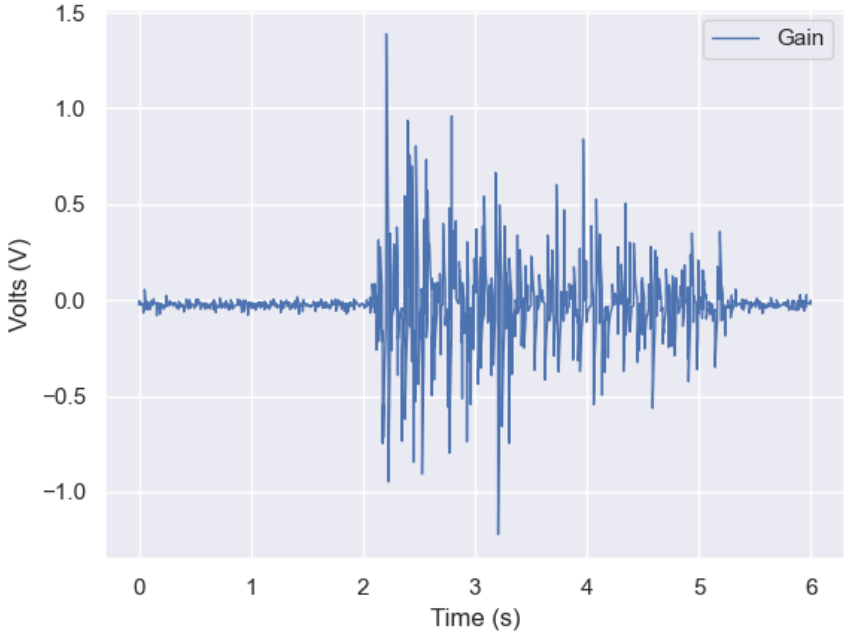

Figure 3.7. Output of the gain stage.

3.3. Filtering

Capacitors C8 and C9 shown in Figure 3.5 act as a highpass filter, letting through only the high frequencies and blocking the small DC value of the signal. This change in the signal can be seen in Figure 3.9, where the red signal clearly shows only the high frequency components of the blue (input) signal. The frequency response of C8 (and C9) can be seen on 3.8, which shows that the cutoff frequency is aproximately 10Hz.

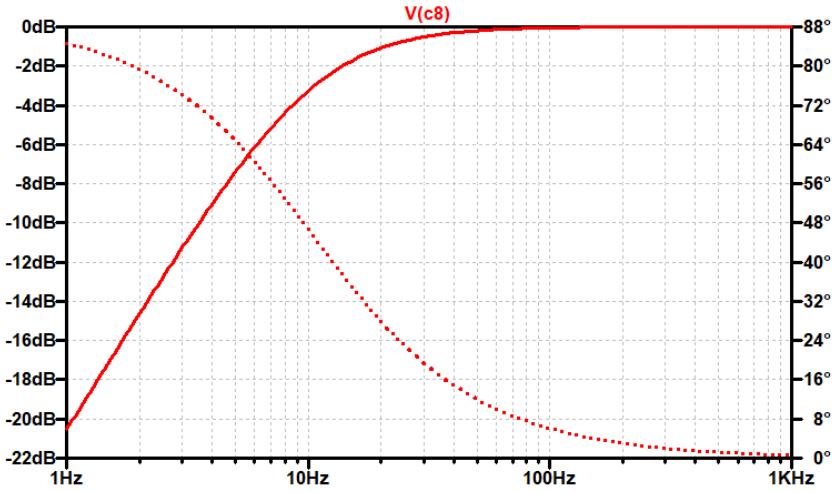

Figure 3.8. Frequency response of capacitor C8 (Figure 3.5)..

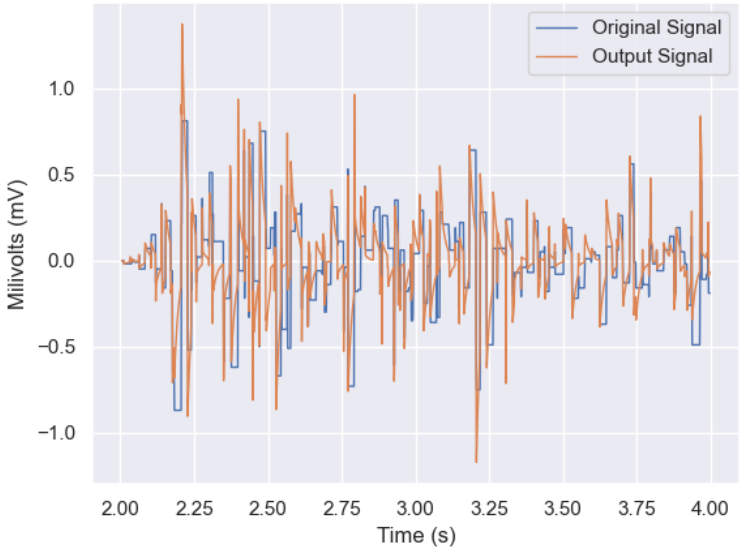

Figure 3.9. Effect of the high-pass filter the capacitor creates. blue - raw EMG signal; red - signal after C8 capacitor in 3.5..

In order to remove high-frequency noise, a low-pass filter is required. Since keeping the gain and a low level of distortion in the signal is necessary, a fourth order Butterworth filter will be sufficient and recommended.

According to Analog Devices, Inc.[20], Butterworth filters are the best compromise between attenuation and phase response. These filters have no ripple in the pass-band

or stop-band (in fact, they are often referred to as "*maximally flat*" filters). Butterworth filters are normalized at $-3\,\mathrm{dB}$ when $\omega_o = 1\,\mathrm{rad/s}$. This means that the poles of the Butterworth filter always fall on the unitary circle in the s plane. The positions of said poles are given by the expression shown in Equation 3.3. This expression creates poles equidistantly spaced in between themselves (the angles between poles are equal).

$$-sin\frac{(2K-1)\pi}{2n} + jcos\frac{(2K-1)\pi}{2n} \qquad K = 1, 2 \ldots, n \tag{3.3}$$

where K is the number associated to the pole pair and n the total number of poles.

In order to build a filter, the Butterworth pole configuration must be implemented into a real-world circuit. To do this, different configurations can be used, being one of the most used the Sallen-Key configuration. A generic schematic of this configuration can be seen on 3.10, in particular, the configuration is of a low-pass second order Sallen-Key filter. The same circuit can be implemented using another different topology, for example the Multiple Feedback Topology (seen on Figure 3.11). For the design of the fourth order Butterworth filter, two Sallen-Key topology filters will be implemented.

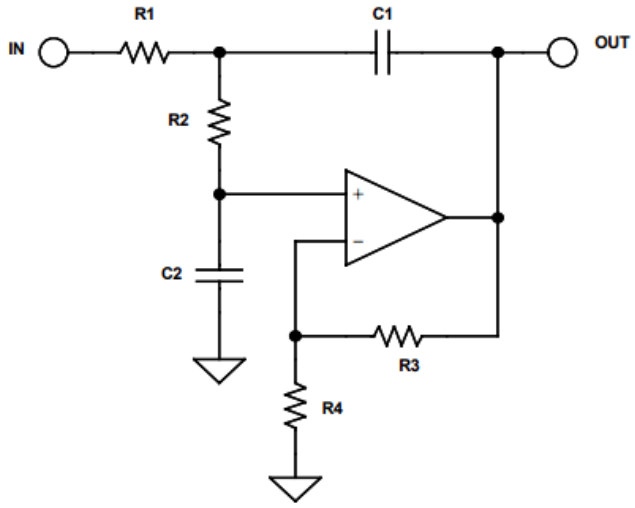

Figure 3.10. Sallen-Key topology of a second order Low-pass Filter.

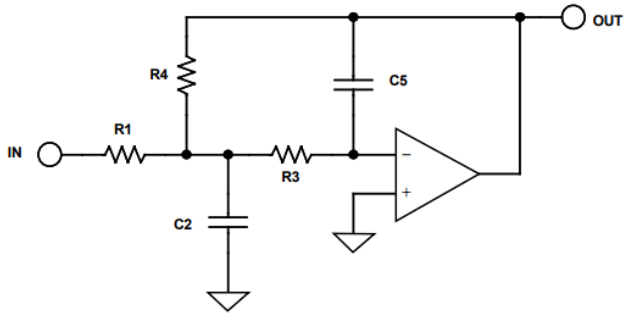

Figure 3.11. Multiple Feedback topology of a second order Low-pass Filter.

The components used in Figure 3.12 are a possible solution to the fourth order Butterworth filter needed. Figure 3.13 represents each stage of the filter. The blue line shows the first stage and how it has a -6 dB at the cut frequency and the red line shows the second stage with a $+3$ dB resonance at that same frequency. This this means that the filter created with both stages put in series will have -3 dB at that frequency.

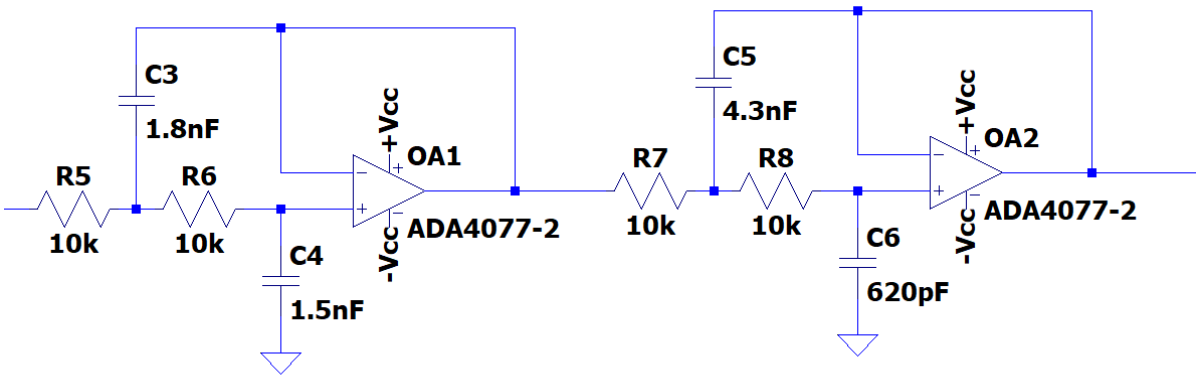

Figure 3.12. Fourth order Lowpass Butterworth filter ($f_c = 10\,\text{kHz}$) using two Sallen-Key stages.

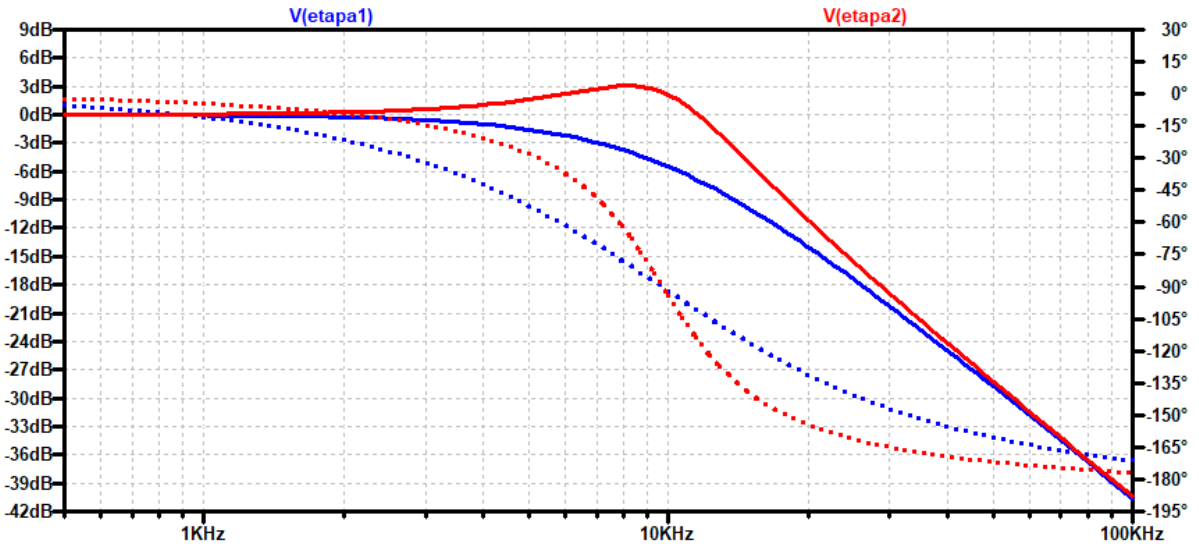

Figure 3.13. Bode diagram of the frequency response of the independent stages in 3.12. Blue continuous line for the gain in dB for the first stage; red continuous line for the gain in dB for the second stage; blue discontinuous line for the phase in degrees; red discontinuous line for the phase in degrees. Frequency is represented in a logarithmic scale.

The results obtained from filtering the signal represented in Figure 3.7 can be seen on Figure 3.14. In this figure, the Gain signal (blue) and the filtered signal (orange) are almost identical due to the lack of noise in the readings from the MYO Thalamic bracelet used to retrieve the EMG signals. Nonetheless, this filter filter will prove useful in future chapters to attenuate noise when using other measurement systems.

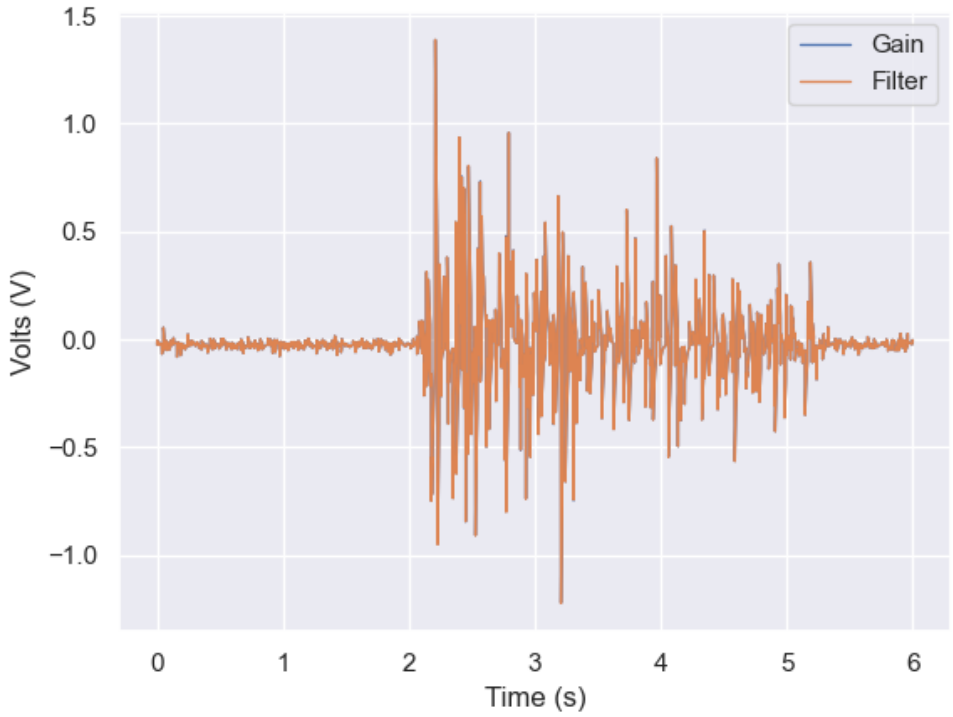

Figure 3.14. Blue signal is that shown on Figure 3.7; Orange signal is the filtered signal (with the filter shown in Figure 3.12).

3.4. Precision Rectifier

According to Coughlin[21], precision full-wave rectifiers deliver an output proportional to the magnitude of the input but not to the polarity of the input. Identically to the absolute value operand in calculus, the output of the circuit can be $+2\,\text{V}$ for either $+2\,\text{V}$ or $-2\,\text{V}$. This type of circuit is quite common when working with signals which are going to be fed into a micro-controller (our case).

The circuit proposed is a full-wave precision rectifier with equal resistors. This is the circuit shown in Figure 3.15. It uses equal resistors (as the name implies) and the input resistance is equal to R.

For positive input signals, diode D1 conducts, making both OA3 and OA4 act as inverters and thus, $V_o = +V_{in}$. When the input signal is negative, D2 conducts and OA4 acts as an inverter, making $V_o = -V_{in}$. Therefore, for either polarity of V_{in}, the output will be positive. The result of simulating this can be seen on Figure 3.16, where the blue signal is the input signal and the orange signal is the rectified signal.

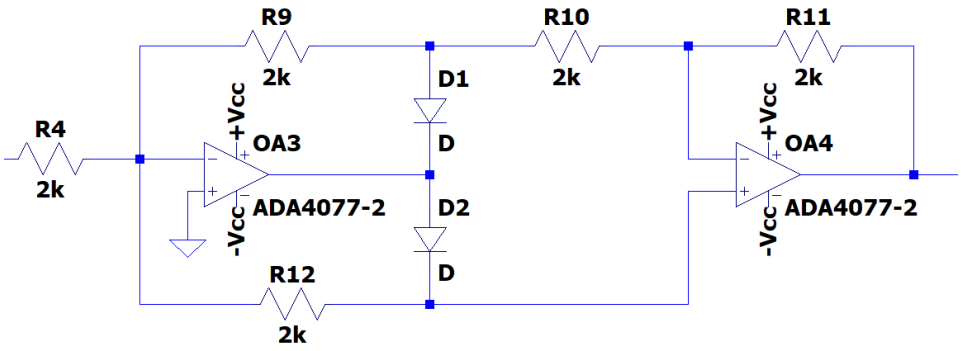

Figure 3.15. Precision Rectifier[21].

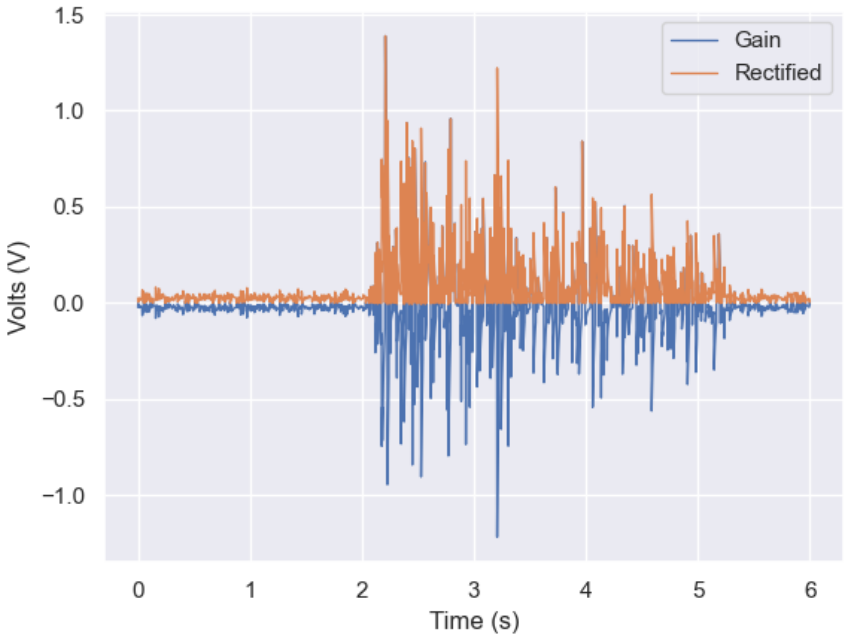

Figure 3.16. Precision Rectifier[21].

3.5. Envelope Detector

As Analog Devices[22] explains, an envelope detector circuit is an electronic circuit which takes a high-frequency signal as the input and outputs the envelope of that signal. There are two main elements:

- Diode - enhances one part of the signal over the other and enables the capacitor to discharge.
- Low-Pass filter - removes the high-frequency component of the signal and "smooths" it. It is usually a simple RC network, where the time constant is $\tau = RC$. This time constant determines the speed of the transient signal. The lower the value of τ, the higher the similarity between the input and output signals.

On top of this, real-world diodes have a voltage drop of around 0,6 V. Since the amplified signal will be close to 2 V, this voltage drop can be considered quite significant and will result in a considerable loss of information. To prevent the voltage drop, a super-diode can be implemented.

According to Keim[23], superdiodes consist of an operational amplifier and a diode in the configuration shown on Figure 3.17. The operational amplifier has a negative feedback and the diode in its output will only be conducting when the voltage V^+ is possitive. When said voltage is negative, the diode will be in its non-conducting state and therefore, no current will flow from the op-amp into the low-pass filter. The op-amp forces the voltage of V^+ to be equal to that of V^-, therefore, this circuit will behave the same way as a diode, without practically any voltage drop. The inconvenience is that the op-amp has to be powered, leading to a higher power consumption than with fully passive components.

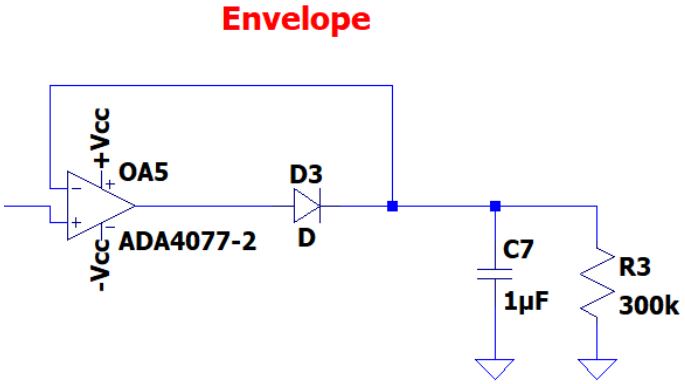

Figure 3.17. Envelope circuit.

On Figure 3.18, different values of τ are compared to see how they will affect the output signal. High values and low values of τ prove useless, due to either being too lax or too restrictive. For our application, a value of $R3 = 200\,\text{k}\Omega - -300\,\text{k}\Omega$ can prove useful.

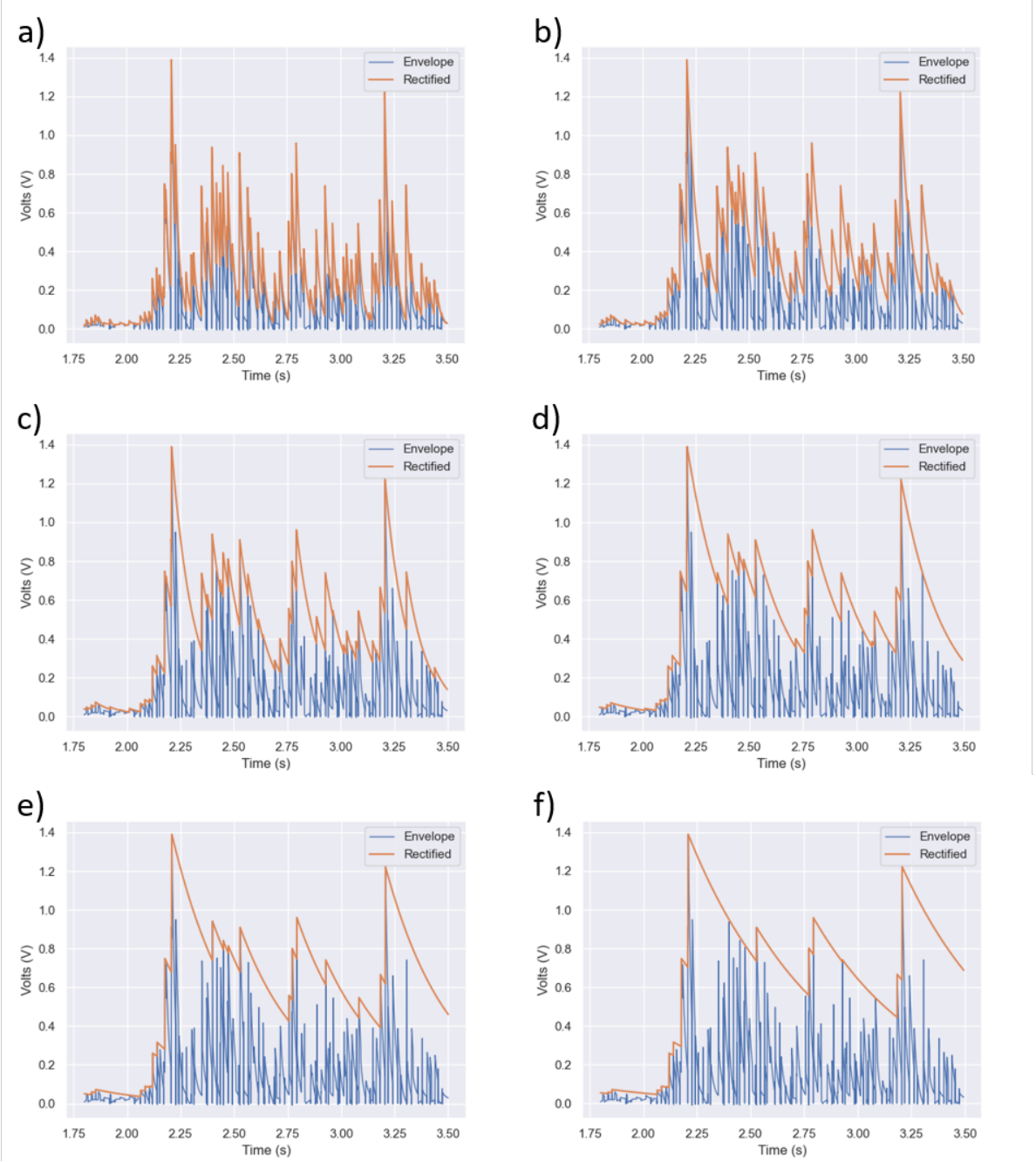

Figure 3.18. Results of the envelope circuit (output - red; input - blue) for different values of R3 (without changing C7 from 1 μF). Values of R3: (a) 20 kΩ, (b) 50 kΩ, (c) 100 kΩ, (d) 200 kΩ, (e) 300 kΩ, (f) 500 kΩ, .

4

Classification

Surface EMG is the easiest and most widespread way to record EMG. As mentioned before (2.1.4), they are not useful when recording small muscles or muscles underneath other bigger muscles because the signals will have too much crosstalk between them. When an EMG signal is amplified and displayed, it tends to represent white noise. White noise is defined in electronics as noise with zero mean, constant variance and uncorrelated in time [24].

4.1. Unprocessed EMG Feature Extraction

Traditional surface EMG pattern recognition methods have been developed under the assumption that EMG signals are stationary or exhibit "stationarity" [25]. This term implies that the statistical properties of the signal remain constant over time. A recognition system which combines transient and steady-state EMG signals would increase the utility of the system, however, it would be much more complex. EMG pattern recognition systems that only consider stationarity would fail to classify EMG patterns specially at the beginning and the end of contractions (dynamic portions). Modern time-frequency and time-scale methods such as short-time Fourier transform and wavelet transform have been used to study the properties of EMG signals[26].

As explained by Phinyomark[25], a combination of simple apporaches using time domain (TD) analysis methods and linear discriminant analysis (LDA) provides performance comparable to those of more complex methods such as the previously mentioned wavelet transform and Artificial Neural Networks (ANN). The performance of TD/LDA is less sensitive to changes and does not require optimization. TD methods in general are not designed to quantify non-stationary signals in a reliable manner. In order to be able to use this method, these features are computed based on the first-order difference of EMG time series, $\delta^{(1)}(t)$, instead of the orginal EMG time series, $x(t)$. EMG features extracted from $\delta^{(1)}(t)$ provide better classification accuracy compared to those of the time series.

One of the most widespread features for classifying EMG signals is the waveform length (WL). Defined as the sum of the absolute value of $\delta^{(1)}(t)$, it can be considered an "extended version" of and integrated EMG (sum of the values of $x(t)$.

Mean absolute value (MAV) and root mean squared (RMS)are often used to estimate EMG amplitude. These features can be modified using the diferentiating technique and recieve the names of difference absolute mean value (DAMV) and difference absolute standard deviation value (DASDV) respectively.

In order to measure frequency domain, many TD features have been proposed by different authors, with the most popular being the Willison amplitude (WAMP) which effectively counts the frequency of motor unit action potentials (MUAPs) firing.

The mathematical expressions for these characteristics can be seen on Table 4.1.

4.2. Preprocessed EMG Feature Extraction

While the features and techniques explained in section 4.1 are valid for unprocessed EMG signals, this is not the case of the project. The EMG signals which will be input into the classifier will ha an analog preprocessing (detailed explanation in chapter 3). Since the output will be quite different from the input signal, most of the techniques mentioned in Table 4.1 are deemed useless for this signal. The reason for doing such preprocessing is to help reduce the computational power needed to process the signal and reduce latency.

With the analog preprocessing used in the project, a new classification method needs to be implemented. The general schematic of an EMG classification method is shown on Figure 4.1.

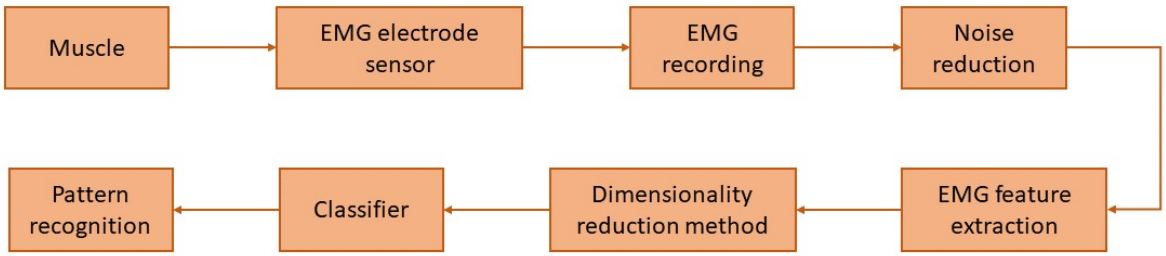

Figure 4.1. General EMG classification block diagram.

Mathematical definitions of existing TD features	
Features extracted from	Features extracted from $\delta^{(1)}(t)$
$IEMG = \sum_{t=1}^{N} \lvert x(t) \rvert$	$WL = \sum_{t=1}^{N-1} \lvert x(t+1) - x(t) \rvert$
$MAV = \frac{1}{N} \sum_{t=1}^{N} \lvert x(t) \rvert$	$DAMV = \frac{1}{N-1} \sum_{t=1}^{N-1} \lvert x(t+1) - x(t) \rvert$
$SSI = \sum_{t=1}^{N} x(t)^2$	$M2 = \sum_{t=1}^{N-1} (x(t+1) - x(t))^2$
$VAR = \frac{1}{N-1} \sum_{t=1}^{N} x(t)^2$	$DVARV = \frac{1}{N-2} \sum_{t=1}^{N-1} (x(t+1) - x(t))^2$
$RMS = \sqrt{\frac{1}{N} \sum_{t=1}^{N} x(t)^2}$	$DASDV = \sqrt{\frac{1}{N-1} \sum_{t=1}^{N-1} (x(t+1) - x(t))^2}$
$MYOP = \frac{1}{N} \sum_{t=1}^{N} [f(\lvert x(t) \rvert)]$	$WAMP = \sum_{t=1}^{N-1} f(\lvert x(t+1) - x(t) \rvert)$
$f(x) = \begin{cases} 1 & \text{if x} \geq \text{threshold} \\ 0 & \text{otherwise} \end{cases}$	

Table 4.1. Mathematical definitions for (IEMG), Waveform Length(WL), Mean Absolute Value (MAV), Difference Absolute Mean Value (DAMV), Signal Strength Indicator(SSI), Second Central Moment (M2), Variance (VAR), Delta Variance (DVARV), Root Mean Square (RMS), Delta Absolute Standard Deviation (DASDV), Myopotentials (MYOP), Willision Amplitude

5 Simulation

5.1. Data acquisition

All of the EMG theory explained before is relatively easy to understand and yields consistent results all around different papers and studies.

To better understand the behaviour of an EMG signal and achieve a preliminary model to begin to work with and reach conclusions, a quick simulation can be used.

The muscle analysed in this case will be the *Flexor Carpi Ulnaris*[1] (seen on Figure 5.1). This muscle is a superficial flexor muscle in the forearm. It is used to flex and adduct the hand. This muscle was chosen due to the easy access to the muscle; being close to the surface; and the fact that it is the most powerful wrist flexor[27].

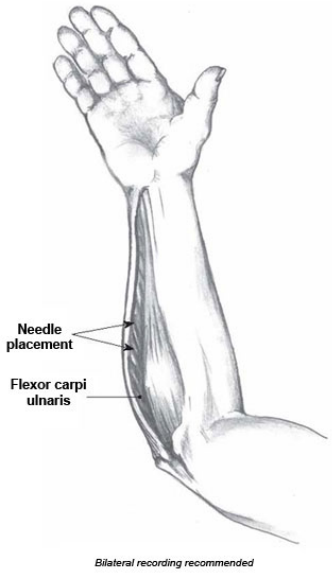

Figure 5.1. Flexor Carpi Ulnaris muscle[28].

[1] onwards refered to as the FCU muscle

Since EMG signals are very small-amplitude signals, measuring them directly is not viable. In order to measure them, the easiest option is to amplify the EMG signal and then simulate the behaviour of the remainder of the circuit to analyse the output and process it.

In order to measure the EMG produced by the FCU muscle, three surface electrodes will be used. And to amplify the signal, the *Muscle Sensor v3* can be of use. The output of the circuit (as analyzed in subsection 1.2.2) yields very little information. The smoothing of the signal is too harsh. However, this device does have an amplifying stage which can be of use. Due to the configuration of the device, when analyzing where it could be viable to tap the amplified EMG signal from, a small inconvenient appeared. This device rectifies the signal and then amplifies it, so the tapped signal will be both amplified and rectified. The spot to which a wire will be soldered (to create the signal tap), can be seen on Figure 5.2.

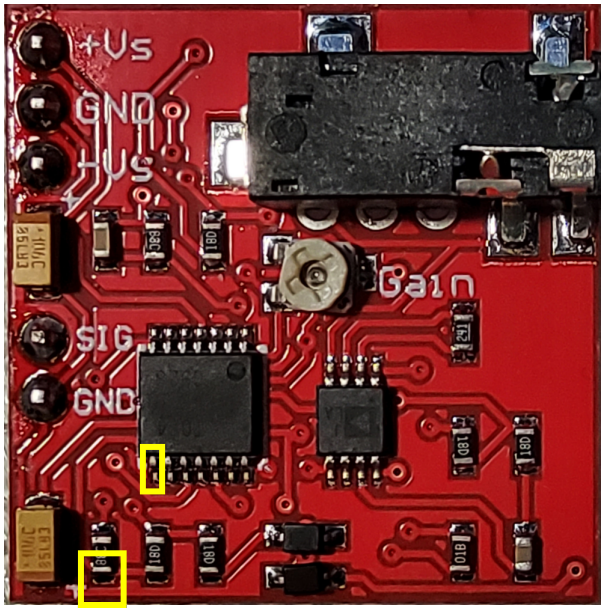

Figure 5.2. Image of the Muscle Sensor v3 sensor showing in yellow two of the possible positions to which a wire can be tapped to extract the signal mentioned.

The electrode placement will be similar to that shown on Figure 5.1. The "neutral" electrode will be located next to the elbow and the "positive" and "negative" will be placed on top of the muscle. Skin surface will be previously thoroughly cleaned and an electrolyte will be used to help reduce unwanted noise and artifacts (as discussed on Chapter 2). An image showing the electrodes placed on the FCU muscle can be seen on Figure 5.3

Three electrodes are used to measure the EMG of the FCU muscle. This is due to the fact that one of them (the green electrode in the case of Figure 5.3) acts as a reference electrode. This electrode provides the "baseline" from which to measure all the electromyographies. In order to achieve a good quality signal, the reference electrode must be located in a point of low muscle activity. In the before mentioned figure, the elbow is chosen as such point, due to the low quantity of muscles in the area.

The other two electrodes (red and black in Figure 5.3) are the active electrodes. These electrodes must be placed on top of the muscle which is going to be measured (in this case the FCU muscle). Having two electrodes allows for the recording to have a higher accuracy (since the potential difference from these two points will be the output). This set-up allows for a more precise and detailed analysis of the muscle's electrical activity compared to using only two electrodes[29].

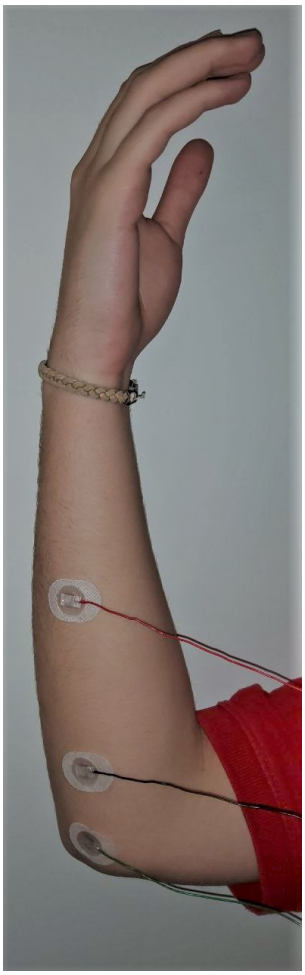

Figure 5.3. Electrodes placed in order to measure the FCU muscle. Green (bottom) is the reference electrode, while red (top) and black (middle) are the active ones.

The signal will be the input of the Muscle Sensor v3 and the measured output will be that of the tapped signal explained on Figure 5.2. This output signal will be used as an input into the simulation, where it will be filtered and taken through the envelope detector circuit.

5.2. Simulating with acquired data

The oscilloscope used to measure the data is the RS PRO RSMSO-2204E. This particular oscilloscope is able to export measurements into a "*.txt*" format which can be processed with MATLAB and/or Python. This model was chosen over others due to it having the possibility to record 3 channels simultaneously (even though two was enough for all measurements) and because it could record files with up to 10 million points. These files were found to be extremely large and took up extensive time periods to be recorded and processed. For this reason, the point count was reduced to 1 million points. This produced a signal with high fidelity, avoided any possible aliasing in the digitalisation and reduced considerably the recording and processing times.

With some simple modifications to the contents of the file (such as adding $5 \times horizontaldivisions$ seconds to the time column to make all times possitive), the text file can be read by LTSpice and used as an input for the simulation. Using the circuit described on Chapter 3, the recorded data from the tapped signal in the Muscle Sensor v3 was processed in different stages.

Firstly, as seen on Figure 5.4, the signal was filtered. In this figure, the blue signal is the output from the Muscle Sensor v3 and the orange signal is the filtered signal using the 10 kHz filter explained on Section 3.3.

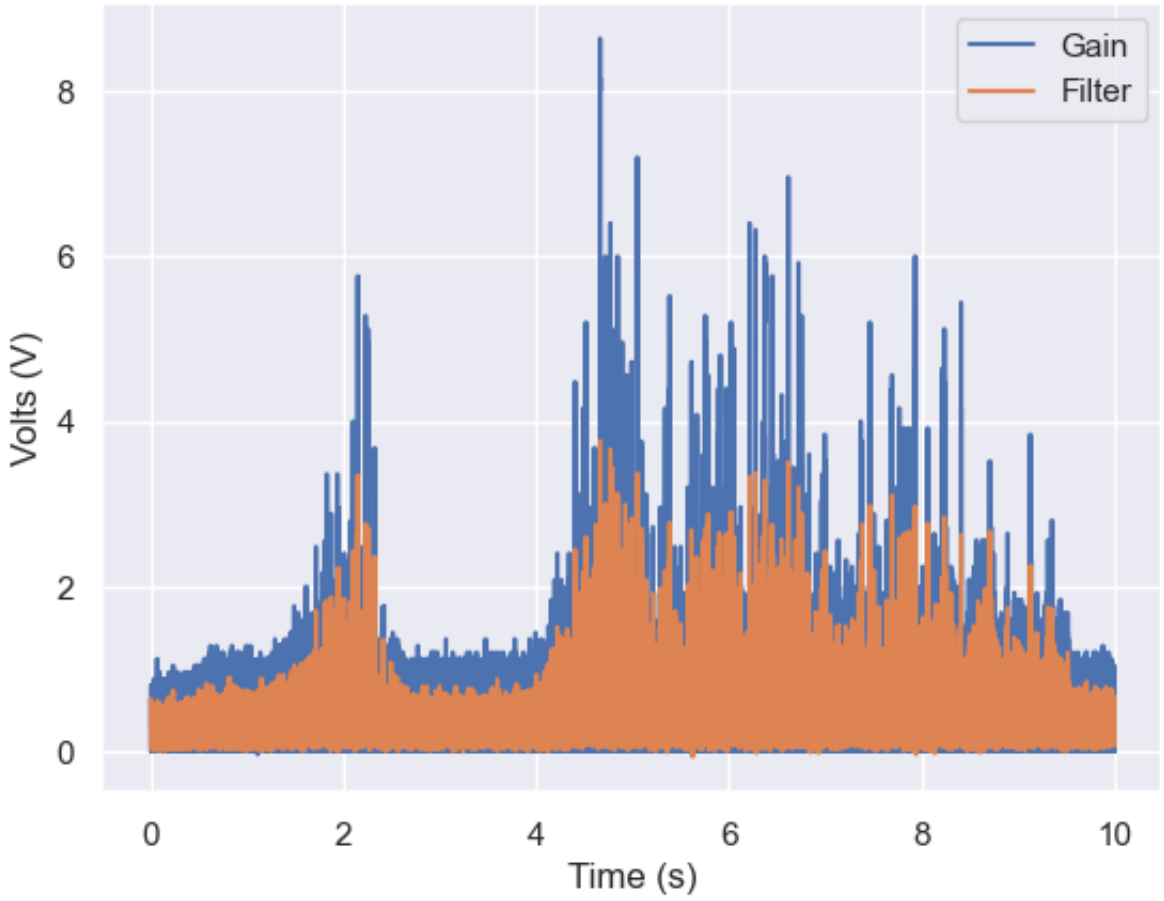

Figure 5.4. Simulation of the filter against recorded data. Filter has a cut frequency of 10 kHz. Blue is the input signal and orange is the filtered signal.

The filtered signal is then input into the envelope detector cirtuit with a $C = 1\,\mu\text{F}$ and $R = 300\,\text{k}\Omega$. The output of this stage is represented on Figure 5.5, where the envelope is represented as the orange signal and the input of the stage in blue (the filtered signal from Figure 5.4.

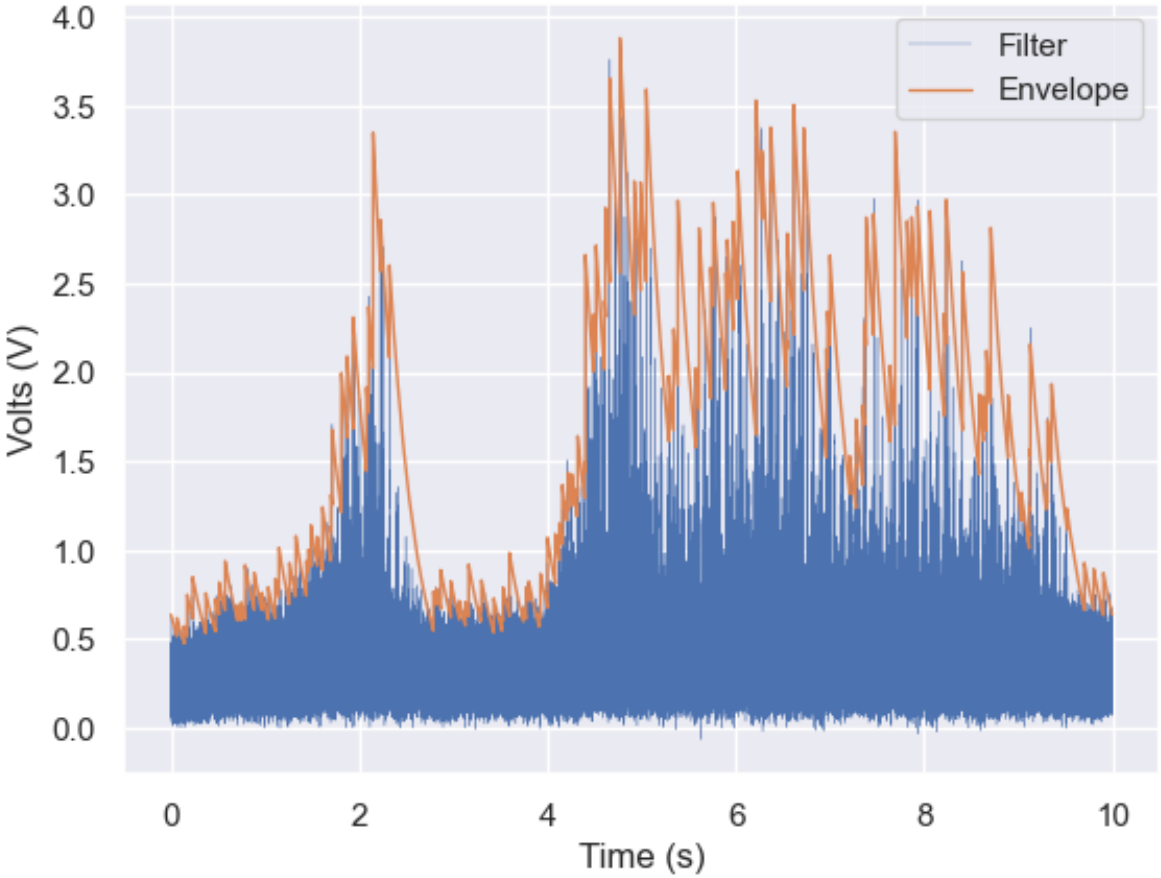

Figure 5.5. Simulation of the envelope detector circuit. Blue is the filtered data input into the stage and orange is the output of the envelope detector. The parameters are: $C = 1\,\mu\text{F}$ and $R = 300\,\text{k}\Omega$.

Analysing the results from this simulation, we can determine that the time constant used in the envelope detector is adequate, since it simplifies the data while maintaining some of its most relevant qualities.

5.3. Classifying simulated data

Reaching the end of the scope of this project, after processing the data in an analog manner, it would be interesting to classify this data digitally. This is why a suitable sampling period must be determined in order to correctly classify this data.

For this purpose, a different measurement was aquired using the oscilloscope mentioned before. While measuring the same muscle (the FCU muscle, see Figure 5.1), the subject performed four increasing levels of strength using a 60 kg gripper and performing the action shown on Figure 5.6.

Figure 5.6. Action performed with grippers in order to record various levels of strength used.

The four levels and the corresponding EMG were recorded and processed following the previous signal. Figure 5.7 shows the output from the Muscle Sensor v3 (blue signal) and the filtered signal (orange). Figure 5.8 shows the filtered signal (blue) and the envelope of the signal (orange).

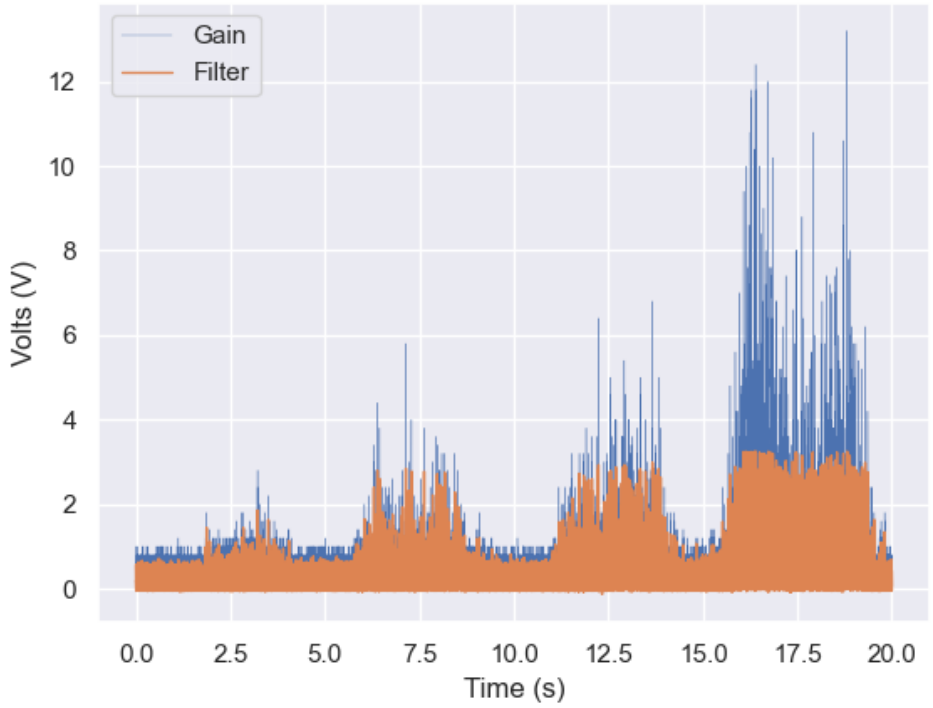

Figure 5.7. Different levels of strength from the FCU muscle. Blue signal is the tapped output from the Muscle Sensor v3; orange signal is the filtered signal.

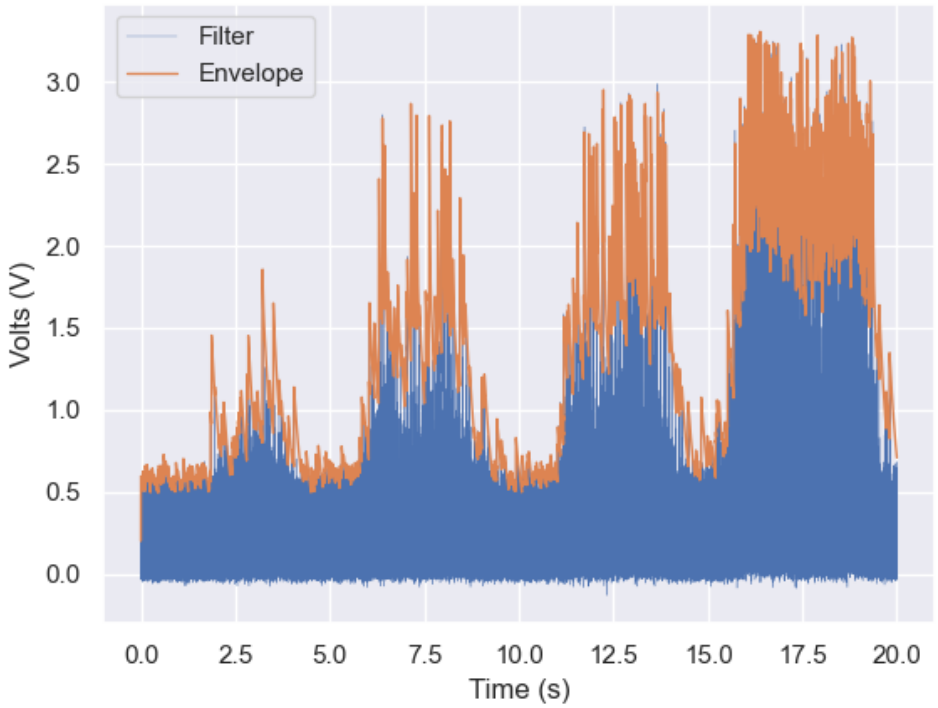

Figure 5.8. Second stage of the simulation for different strength levels. Blue signal is the filtered signal; orange signal is the envelope of the filtered signal.

From this point onwards, the signal is going to be digital, therefore a suitable sampling time must be selected. Sampling times must be as big as possible to reduce power consumption. A large sampling time helps to process the data, since more complex calculations can be done with it (since there is more time available in between measurements). However, large sampling times tend to produce slow responses in digital systems, therefore a compromise must be achieved between how fast we want to answer to a stimulus and the power we are willing to consume.

A possible solution could be to go full-blast and process data in almost real-time and read as fast as our micro-controller would let us. This would yield a fantastic response time with the downside of having an extremely high power consumption. The other extreme would be to read the signal every large period of time. This would consume very little power, but the response would be slow or even non-existent (if for example in between reads the muscle contracted and relaxed back to its original position, there would be no recording of this).

In order to analyse a suitable sampling time (or T_s), the data from Figure 5.8 was processed using a simple MATLAB script. By using the *movvar*[30] and the *movmean*[31] functions, a moving variance and mean (respectively) can be created. For this particular example, since there are close to 10 million data points after the LTSpice simulation, these moving mean and variance were calculated using only 300 thousand of those points at a time (around 0.2 seconds of simulation, or 1% of the total simulation time).

These two characteristics are the ones going to be used in this simple model to determine the intensity of the muscle activity. By using a simple formula like the one on Equation 5.1, a $VALUE$ can be calculated. This $VALUE$ will be the input of our classifier. δ_1 and δ_2 represent the weights of each variable. In this particular case, a value of $\delta_1 = 1$ and $\delta_2 = 3$ were found suitable. However, these values do not guarantee the correct behaviour of this simplified model for all scenarios, just the one analysed.

$$VALUE = MEAN \times \delta_1 + VARIANCE \times \delta_2 \tag{5.1}$$

By using the same classifier function and changing the sample time, the graphs represented on Figure 5.9 are created. This figure shows how decreasing the sampling time affects the classifier. In this particular case, the sample times selected were 1 s, 100 ms, 10 ms, 1 ms and 100 μs.

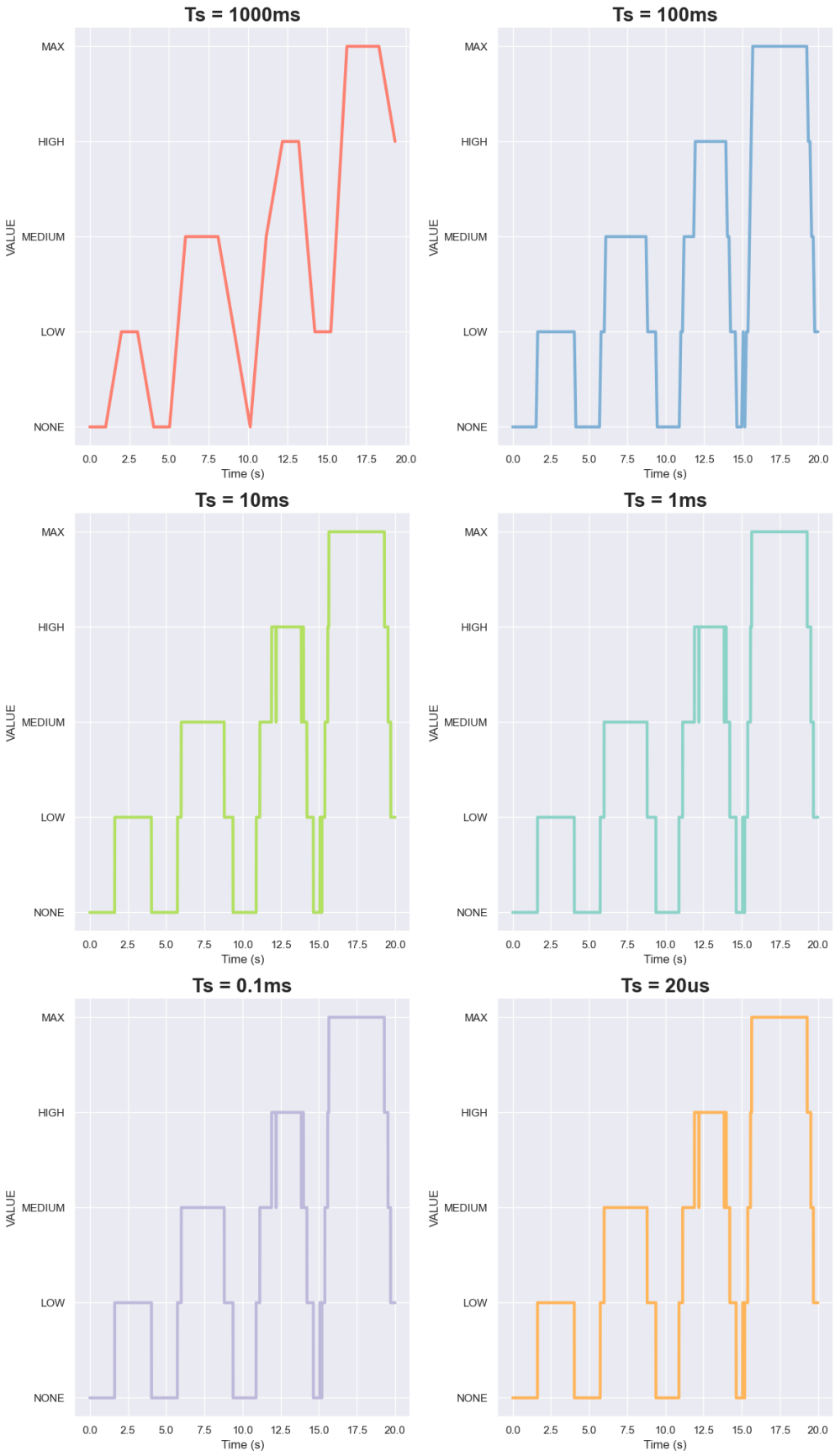

Figure 5.9. Level the classifier classified the input signal as for different sampling times (from left to right, up then down: 1 s, 100 ms, 10 ms, 1 ms, 100 μs and the original data sampling time (which is 20 μs)).

By looking at Figure 5.9, it is clear that sample times lower than 100 ms yield a very similar result, being very hard to distinguish them for sample times lower than 10 ms.

According to research carried out by [32], the average human reaction time is 220 ms for simple reactions. If we were to use a sampling time of 100 ms, this would mean that any action performed by the digital system would have a delay of 45 % of the total reaction time. This delay when implemented into a prosthesis could be uncomfortable and cause frustration on the patient. However, since decreasing the sampling time over this value has no practical effect, a more suitable sampling time could be of 20 ms (around 10 % of the total reaction time of the signal).

6

Conclusion

The main goal of this project is to reduce the quantity of data processed by the micro-controller in which the digital classification algorithm takes place. This data must be sufficient to reliably classify the EMG signals into their correct strength value without consuming excessive amounts of power. The final goal is to have the digital measuring interface implanted under the skin, so minimizing this data-transfer will help to keep the temperatures of this hardware under control.

The data sampled with the oscilloscope has 1 Million samples in 20 s, this means that the sampling time is 20 μs. This sampling time is very high and needs to be reduced.

Taking into consideration the conclusions yielded from the analysis of Figure 5.9 in Chapter 5, the sampling time can be reduced from 20 μs to 20 ms.

If the data is measured using 8 bits (1 bytes), the total data transferred measuring every 20 μs can be calculated using the expression shown on Equation 6.1.

$$DATA_{20\mu s} = \frac{8bits}{20\mu s} \times \frac{10^6 \mu s}{1s} = 400{,}000\,\text{bits/s} \tag{6.1}$$

However, when the sampling time is 20 ms, the total quantity of data transferred is shown on Equation 6.2.

$$DATA_{20ms} = \frac{8bits}{20ms} \times \frac{10^3 ms}{1s} = 400\,\text{bits/s} \tag{6.2}$$

Therefore, by reducing the sampling time of the signal, the amount of data processed by the digital system is 1000 times less than it would have been if the original oscilloscope's data points were to be taken into account. All this, with little-to-none perceivable data loss.

6.1. Sustainable Development Goals alignment

The Sustainable Development Goals (SDGs)[33] originated in 2015 when the United Nations set 17 global goals. The goals are universal, integrated and transformative. They aim to cover the social, economic and environmental aspects of most aspects of our development. Most SDGs are aimed towards developing countries (No poverty, health and well-being, zero hunger, etc...). The main SDGs taken into consideration in this project are:

SDG 3 - Good Health and Well-Being[34]: "Ensure healthy lives and promote well-being for all at all ages". There are many objectives alongside this SDG. It covers from reducing the global maternal mortality, to end several epidemics (AIDS, tuberculosis, etc...). This project covers another aspect of Health and Well-Being. It will not solve a huge global issue, its purpose is to solve problems for a selected group of people with a specific injury. The main goal is for these people to regain mobility in their arms, increasing their well-being and ensuring they carry out a normal life as they had once done.

SDG 9 - Industries, Innovation and Infrastructure[35]: "...foster innovation". Investigating and developing this technology can lead into a new way to treat permanent injuries. Innovating in this field can lead to unexpected consequences. Maybe the research done in this field oriented toward this technology can lead to another discovery in a vastly different application.

A

ANNEX

A.1. AD8422 datasheet

ANALOG DEVICES

High Performance, Low Power, Rail-to-Rail Precision Instrumentation Amplifier

Data Sheet **AD8422**

FEATURES

Low power: 330 µA maximum quiescent current
Rail-to-rail output
Low noise and distortion
8 nV/√Hz maximum input voltage noise at 1 kHz
0.15 µV p-p RTI noise (G = 100)
0.5 ppm nonlinearity with 2 kΩ load (G = 1)
Excellent ac specifications
80 dB minimum CMRR at 7 kHz (G = 1)
2.2 MHz bandwidth (G = 1)
High precision dc performance (AD8422BRZ)
150 dB minimum CMRR (G = 1000)
0.04% maximum gain error (G = 1000)
0.3 µV/°C maximum input offset drift
0.5 nA maximum input bias current
Wide supply range
3.6 V to 36 V single supply
±1.8 V to ±18 V dual supply
Input overvoltage protection: 40 V from opposite supply
Gain range: 1 to 1000

APPLICATIONS

Medical instrumentation
Industrial process controls
Strain gages
Transducer interfaces
Precision data acquisition systems
Channel-isolated systems
Portable instrumentation

CONNECTION DIAGRAM

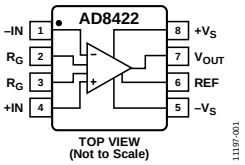

Figure 1. 8-Lead MSOP (RM), 8-Lead SOIC (R)

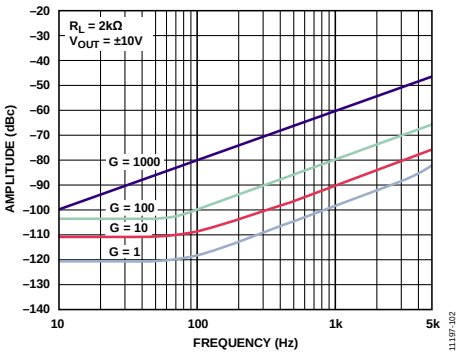

Figure 2. Total Harmonic Distortion vs. Frequency

GENERAL DESCRIPTION

The AD8422 is a high precision, low power, low noise, rail-to-rail instrumentation amplifier that delivers the best performance per unit microampere in the industry. The AD8422 processes signals with ultralow distortion performance that is load independent over its full output range.

The AD8422 is the third generation development of the industry-standard AD620. The AD8422 employs new process technologies and design techniques to achieve higher dynamic range and lower errors than its predecessors, while consuming less than one-third of the power. The AD8422 uses the high performance pinout introduced by the AD8221.

Very low bias current makes the AD8422 error-free with high source impedance, allowing multiple sensors to be multiplexed to the inputs. Low voltage noise and low current noise make the AD8422 an ideal choice for measuring a Wheatstone bridge.

The wide input range and rail-to-rail output of the AD8422 bring all of the benefits of a high performance in-amp to single-supply applications. Whether using high or low supply voltages, the power savings make the AD8422 an excellent choice for high channel count or power sensitive applications on a very tight error budget.

The AD8422 uses robust input protection that ensures reliability without sacrificing noise performance. The AD8422 has high ESD immunity, and the inputs are protected from continuous voltages up to 40 V from the opposite supply rail.

A single resistor sets the gain from 1 to 1000. The reference pin can be used to apply a precise offset to the output voltage.

The AD8422 is specified from −40°C to +85°C and has typical performance curves to 125°C. It is available in 8-lead MSOP and 8-lead SOIC packages.

SPECIFICATIONS

SOIC PACKAGE

V_S = ±15 V, V_{REF} = 0 V, T_A = 25°C, G = 1, R_L = 2 kΩ, unless otherwise noted.

Table 1.

Parameter	Test Conditions/ Comments	AD8422ARZ Min	AD8422ARZ Typ	AD8422ARZ Max	AD8422BRZ Min	AD8422BRZ Typ	AD8422BRZ Max	Unit
COMMON-MODE REJECTION RATIO								
CMRR DC to 60 Hz with 1 kΩ Source Imbalance	V_{CM} = −10 V to +10 V							
G = 1		86			94			dB
G = 10		106			114			dB
G = 100		126			134			dB
G = 1000		146			150			dB
Over Temperature, G=1	T = −40°C to +85°C	83			89			dB
CMRR at 7 kHz	V_{CM} = −10 V to +10 V							
G = 1		80			80			dB
G = 10		90			95			dB
G = 100		100			100			dB
G = 1000		100			100			dB
NOISE[1]								
Voltage Noise, 1 kHz								
Input Voltage Noise, e_{NI}	V_{IN+}, V_{IN-}, V_{REF} = 0 V			8			8	nV/√Hz
Output Voltage Noise, e_{NO}				80			80	nV/√Hz
Peak to Peak, RTI	f = 0.1 Hz to 10 Hz							
G = 1			2			2		µV p-p
G = 10			0.5			0.5		µV p-p
G = 100 to 1000			0.15			0.15		µV p-p
Current Noise	f = 1 kHz		90			90	110	fA/√Hz
	f = 0.1 Hz to 10 Hz		8			8		pA p-p
VOLTAGE OFFSET[2]								
Input Offset, V_{OSI}	V_S = ±1.8 V to ±15 V			60			25	µV
Over Temperature	T = −40°C to +85°C			70			40	µV
Average Temperature Coefficient				0.4			0.3	µV/°C
Output Offset, V_{OSO}	V_S = ±1.8 V to ±15 V			300			150	µV
Over Temperature	T = −40°C to +85°C			500			300	µV
Average Temperature Coefficient				5			2	µV/°C
Offset RTI vs. Supply (PSR)	V_S = ±1.8 V to ±18 V							
G = 1		90	110		100	120		dB
G = 10		110	130		120	140		dB
G = 100		124	150		140	160		dB
G = 1000		130	150		140	160		dB
INPUT CURRENT								
Input Bias Current	V_S = ±1.8 V to ±15 V		0.5	1		0.2	0.5	nA
Over Temperature	T = −40°C to +85°C			2			1	nA
Average Temperature Coefficient			4			4		pA/°C
Input Offset Current	V_S = ±1.8 V to ±15 V		0.2	0.3		0.1	0.15	nA
Over Temperature	T = −40°C to +85°C			0.8			0.3	nA
Average Temperature Coefficient			1			1		pA/°C

Parameter	Test Conditions/ Comments	AD8422ARZ Min	AD8422ARZ Typ	AD8422ARZ Max	AD8422BRZ Min	AD8422BRZ Typ	AD8422BRZ Max	Unit
REFERENCE INPUT								
R_{IN}			20			20		kΩ
I_{IN}	V_{IN+}, V_{IN-}, V_{REF} = 0 V		35	50		35	50	μA
Voltage Range		$-V_S$		$+V_S$	$-V_S$		$+V_S$	V
Gain to Output			1			1		V/V
DYNAMIC RESPONSE								
Small Signal −3 dB Bandwidth								
G = 1			2200			2200		kHz
G = 10			850			850		kHz
G = 100			120			120		kHz
G = 1000			12			12		kHz
Settling Time 0.01%	10 V step							
G = 1			13			13		μs
G = 10			13			13		μs
G = 100			12			12		μs
G = 1000			80			80		μs
Settling Time 0.001%	10 V step							
G = 1			15			15		μs
G = 10			15			15		μs
G = 100			15			15		μs
G = 1000			160			160		μs
Slew Rate	G = 1 to 100	0.8			0.8			V/μs
GAIN[3]	G = 1 + (19.8 kΩ/R_G)							
Gain Range		1		1000	1		1000	V/V
Gain Error	V_{OUT} ± 10 V							
G = 1				0.03			0.01	%
G = 10				0.2			0.04	%
G = 100				0.2			0.04	%
G = 1000				0.2			0.04	%
Gain Nonlinearity	V_{OUT} = −10 V to +10 V							
G = 1	R_L = 2 kΩ		0.5	5		0.5	5	ppm
G = 10			2	5		2	5	ppm
G = 100			4	10		4	10	ppm
G = 1000			10	20		10	20	ppm
Gain vs. Temperature								
G = 1				5			1	ppm/°C
G > 1				−80			−80	ppm/°C
INPUT								
Input Impedance								
Differential			200||2			200||2		GΩ||pF
Common Mode			200||2			200||2		GΩ||pF
Input Operating Voltage Range[4]	V_S = ±1.8 V to ±18 V	$-V_S$ + 1.2		$+V_S$ − 1.1	$-V_S$ + 1.2		$+V_S$ − 1.1	V
Over Temperature	T = −40°C to +85°C	$-V_S$ + 1.2		$+V_S$ − 1.2	$-V_S$ + 1.2		$+V_S$ − 1.2	V
OUTPUT								
Output Swing, R_L = 10 kΩ	V_S = ±15 V	$-V_S$ + 0.2		$+V_S$ − 0.2	$-V_S$ + 0.2		$+V_S$ − 0.2	V
Over Temperature	T = −40°C to +85°C	$-V_S$ + 0.25		$+V_S$ − 0.25	$-V_S$ + 0.25		$+V_S$ − 0.25	V
Output Swing, R_L = 10 kΩ	V_S = ±1.8 V	$-V_S$ + 0.12		$+V_S$ − 0.12	$-V_S$ + 0.12		$+V_S$ − 0.12	V
Over Temperature	T = −40°C to +85°C	$-V_S$ + 0.13		$+V_S$ − 0.13	$-V_S$ + 0.13		$+V_S$ − 0.13	V
Output Swing, R_L = 2 kΩ	V_S = ±15 V	$-V_S$ + 0.25		$+V_S$ − 0.25	$-V_S$ + 0.25		$+V_S$ − 0.25	V
Over Temperature[5]	T = −40°C to +85°C	$-V_S$ + 0.3		$+V_S$ − 1.4	$-V_S$ + 0.3		$+V_S$ − 1.4	V
Output Swing, R_L = 2 kΩ	V_S = ±1.8 V	$-V_S$ + 0.15		$+V_S$ − 0.15	$-V_S$ + 0.15		$+V_S$ − 0.15	V
Over Temperature	T = −40°C to +85°C	$-V_S$ + 0.2		$+V_S$ − 0.2	$-V_S$ + 0.2		$+V_S$ − 0.2	V
Short-Circuit Current			20			20		mA

Parameter	Test Conditions/ Comments	AD8422ARZ Min	AD8422ARZ Typ	AD8422ARZ Max	AD8422BRZ Min	AD8422BRZ Typ	AD8422BRZ Max	Unit
POWER SUPPLY								
Operating Range	Dual-supply operation	±1.8		±18	±1.8		±18	V
	Single-supply operation	3.6		36	3.6		36	V
Quiescent Current			300	330		300	330	µA
Over Temperature	T = −40°C to +85°C			400			400	µA
TEMPERATURE RANGE								
Specified Performance		−40		+85	−40		+85	°C
Operating Range[6]		−40		+125	−40		+125	°C

[1] Total RTI noise = $\sqrt{e_{NI}^2 + (e_{NO}/G)^2}$
[2] Total RTI V_{OS} = (V_{OSI}) + (V_{OSO}/G).
[3] Gain does not include the effects of the external resistor, R_G.
[4] One input grounded. G = 1.
[5] Output current limited at cold temperatures. See Figure 35.
[6] See Typical Performance Characteristics for expected operation between 85°C and 125°C.

MSOP PACKAGE

V_S = ±15 V, V_{REF} = 0 V, T_A = 25°C, G = 1, R_L = 2 kΩ, unless otherwise noted.

Table 2.

Parameter	Test Conditions/ Comments	AD8422ARMZ Min	AD8422ARMZ Typ	AD8422ARMZ Max	AD8422BRMZ Min	AD8422BRMZ Typ	AD8422BRMZ Max	Unit
COMMON-MODE REJECTION RATIO								
CMRR DC to 60 Hz with 1 kΩ Source Imbalance	V_{CM} = −10 V to +10 V							
G = 1		86			90			dB
G = 10		106			110			dB
G = 100		126			130			dB
G = 1000		146			150			dB
Over Temperature, G = 1	T = −40°C to +85°C	83			86			
CMRR at 7 kHz	V_{CM} = −10 V to +10 V							
G = 1		80			80			dB
G = 10		90			95			dB
G = 100		100			100			dB
G = 1000		100			100			dB
NOISE[1]								
Voltage Noise, 1 kHz								
Input Voltage Noise, e_{NI}	V_{IN+}, V_{IN-}, V_{REF} = 0 V			8			8	nV/√Hz
Output Voltage Noise, e_{NO}				80			80	nV/√Hz
Peak to Peak, RTI	f = 0.1 Hz to 10 Hz							
G = 1			2			2		µV p-p
G = 10			0.5			0.5		µV p-p
G = 100 to 1000			0.15			0.15		µV p-p
Current Noise	f = 1 kHz		90			90	110	fA/√Hz
	f = 0.1 Hz to 10 Hz		8			8		pA p-p
VOLTAGE OFFSET[2]								
Input Offset, V_{OSI}	V_S = ±1.8 V to ±15 V			70			50	µV
Over Temperature	T = −40°C to +85°C			110			75	µV
Average Temperature Coefficient				0.6			0.4	µV/°C
Output Offset, V_{OSO}	V_S = ±1.8 V to ±15 V			300			150	µV
Over Temperature	T = −40°C to +85°C			500			300	µV
Average Temperature Coefficient				5			2	µV/°C

Parameter	Test Conditions/ Comments	AD8422ARMZ Min	AD8422ARMZ Typ	AD8422ARMZ Max	AD8422BRMZ Min	AD8422BRMZ Typ	AD8422BRMZ Max	Unit
Offset RTI vs. Supply (PSR)	V_S = ±1.8 V to ±18 V							
G = 1		90	110		100	120		dB
G = 10		110	130		120	140		dB
G = 100		124	150		140	160		dB
G = 1000		130	150		140	160		dB
INPUT CURRENT								
Input Bias Current	V_S = ±1.8 V to ±15 V		0.5	1		0.2	0.5	nA
Over Temperature	T = −40°C to +85°C			2			1	nA
Average Temperature Coefficient			4			4		pA/°C
Input Offset Current	V_S = ±1.8 V to ±15 V		0.2	0.3		0.1	0.15	nA
Over Temperature	T = −40°C to +85°C			0.8			0.3	nA
Average Temperature Coefficient			1			1		pA/°C
REFERENCE INPUT								
R_{IN}			20			20		kΩ
I_{IN}	V_{IN+}, V_{IN-}, V_{REF} = 0 V		35	50		35	50	µA
Voltage Range		$-V_S$		$+V_S$	$-V_S$		$+V_S$	V
Gain to Output			1			1		V/V
DYNAMIC RESPONSE								
Small Signal −3 dB Bandwidth								
G = 1			2200			2200		kHz
G = 10			850			850		kHz
G = 100			120			120		kHz
G = 1000			12			12		kHz
Settling Time 0.01%	10 V step							
G = 1			13			13		µs
G = 10			13			13		µs
G = 100			12			12		µs
G = 1000			80			80		µs
Settling Time 0.001%	10 V step							
G = 1			15			15		µs
G = 10			15			15		µs
G = 100			15			15		µs
G = 1000			160			160		µs
Slew Rate	G = 1 to 100	0.8			0.8			V/µs
GAIN[3]	G = 1 + (19.8 kΩ/R_G)							
Gain Range		1		1000	1		1000	V/V
Gain Error	V_{OUT} ± 10 V							
G = 1				0.03			0.01	%
G = 10				0.2			0.04	%
G = 100				0.2			0.04	%
G = 1000				0.2			0.04	%
Gain Nonlinearity	V_{OUT} = −10 V to +10 V							
G = 1	R_L = 2 kΩ		0.5	5		0.5	5	ppm
G = 10			2	5		2	5	ppm
G = 100			4	10		4	10	ppm
G = 1000			10	20		10	20	ppm
Gain vs. Temperature								
G = 1				5			1	ppm/°C
G > 1				−80			−80	ppm/°C

Parameter	Test Conditions/ Comments	AD8422ARMZ Min	AD8422ARMZ Typ	AD8422ARMZ Max	AD8422BRMZ Min	AD8422BRMZ Typ	AD8422BRMZ Max	Unit
INPUT								
Input Impedance								
Differential			200||2			200||2		GΩ||pF
Common Mode			200||2			200||2		GΩ||pF
Input Operating Voltage Range[4]	V_S = ±1.8 V to ±18 V	$-V_S$ + 1.2		$+V_S$ − 1.1	$-V_S$ + 1.2		$+V_S$ − 1.1	V
Over Temperature	T = −40°C to +85°C	$-V_S$ + 1.2		$+V_S$ − 1.2	$-V_S$ + 1.2		$+V_S$ − 1.2	V
OUTPUT								
Output Swing, R_L = 10 kΩ	V_S = ±15 V	$-V_S$ + 0.2		$+V_S$ − 0.2	$-V_S$ + 0.2		$+V_S$ − 0.2	V
Over Temperature	T = −40°C to +85°C	$-V_S$ + 0.25		$+V_S$ − 0.25	$-V_S$ + 0.25		$+V_S$ − 0.25	V
Output Swing, R_L = 10 kΩ	V_S = ±1.8 V	$-V_S$ + 0.12		$+V_S$ − 0.12	$-V_S$ + 0.12		$+V_S$ − 0.12	V
Over Temperature	T = −40°C to +85°C	$-V_S$ + 0.13		$+V_S$ − 0.13	$-V_S$ + 0.13		$+V_S$ − 0.13	V
Output Swing, R_L = 2 kΩ	V_S = ±15 V	$-V_S$ + 0.25		$+V_S$ − 0.25	$-V_S$ + 0.25		$+V_S$ − 0.25	V
Over Temperature[5]	T = −40°C to +85°C	$-V_S$ + 0.3		$+V_S$ − 1.4	$-V_S$ + 0.3		$+V_S$ − 1.4	V
Output Swing, R_L = 2 kΩ	V_S = ±1.8 V	$-V_S$ + 0.15		$+V_S$ − 0.15	$-V_S$ + 0.15		$+V_S$ − 0.15	V
Over Temperature	T = −40°C to +85°C	$-V_S$ + 0.2		$+V_S$ − 0.2	$-V_S$ + 0.2		$+V_S$ − 0.2	V
Short-Circuit Current			20			20		mA
POWER SUPPLY								
Operating Range	Dual-supply operation	±1.8		±18	±1.8		±18	V
	Single-supply operation	3.6		36	3.6		36	V
Quiescent Current			300	330		300	330	µA
Over Temperature	T = −40°C to +85°C			400			400	µA
TEMPERATURE RANGE								
Specified Performance		−40		+85	−40		+85	°C
Operating Range[6]		−40		+125	−40		+125	°C

[1] Total RTI Noise = $\sqrt{e_{NI}^2 + (e_{NO}/G)^2}$
[2] Total RTI V_{OS} = (V_{OSI}) + (V_{OSO}/G).
[3] Gain does not include the effects of the external resistor, R_G.
[4] One input grounded. G = 1.
[5] Output current limited at cold temperatures. See Figure 35.
[6] See Typical Performance Characteristics for expected operation between 85°C and 125°C.

ABSOLUTE MAXIMUM RATINGS

Table 3.

Parameter	Rating
Supply Voltage	±1.8 V to ±18 V
Output Short-Circuit Current Duration	Indefinite
Maximum Voltage at –IN or +IN[1]	$-V_S$ + 40 V
Minimum Voltage at –IN or +IN	$+V_S$ – 40 V
Maximum Voltage at REF	$\pm V_S$ ± 0.3 V
Storage Temperature Range	–65°C to +150°C
Operating Temperature Range	–40°C to +125°C
Maximum Junction Temperature	150°C
ESD	
Human Body Model	3 kV
Charge Device Model	1.25 kV
Machine Model	100 V

[1] For voltages beyond these limits, use input protection resistors. See the Theory of Operation section for more information.

Stresses above those listed under Absolute Maximum Ratings may cause permanent damage to the device. This is a stress rating only; functional operation of the device at these or any other conditions above those indicated in the operational section of this specification is not implied. Exposure to absolute maximum rating conditions for extended periods may affect device reliability.

THERMAL RESISTANCE

θ_{JA} is specified for a device in free air using a 4-layer JEDEC printed circuit board (PCB).

Table 4.

Package	θ_{JA}	Unit
8-Lead SOIC	100	°C/W
8-Lead MSOP	162	°C/W

ESD CAUTION

ESD (electrostatic discharge) sensitive device. Charged devices and circuit boards can discharge without detection. Although this product features patented or proprietary protection circuitry, damage may occur on devices subjected to high energy ESD. Therefore, proper ESD precautions should be taken to avoid performance degradation or loss of functionality.

PIN CONFIGURATION AND FUNCTION DESCRIPTIONS

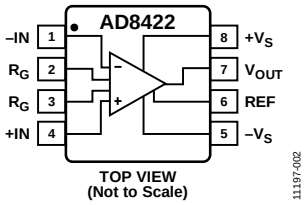

Figure 3. Pin Configuration

Table 5. Pin Function Descriptions

Pin No.	Mnemonic	Description
1	–IN	Negative Input Terminal.
2, 3	R_G	Gain Setting Terminals. Place resistor across the R_G pins to set the gain. G = 1 + (19.8 kΩ/R_G).
4	+IN	Positive Input Terminal.
5	$-V_S$	Negative Power Supply Terminal.
6	REF	Reference Voltage Terminal. Drive this terminal with a low impedance voltage source to level shift the output.
7	V_{OUT}	Output Terminal.
8	$+V_S$	Positive Power Supply Terminal.

A.2. Muscle Sensor v3 datasheet

Muscle Sensor v3

Advancer Technologies
Advancing the Future

Three-lead Differential Muscle/Electromyography Sensor for Microcontroller Applications

FEATURES

- Small Form Factor (1inch X 1inch)
- Specially Designed For Microcontrollers
- Adjustable Gain – Improved Ruggedness
- New On-board 3.5mm Cable Port
- Pins Fit Easily on Standard Breadboards

APPLICATIONS

- Video games
- Robots
- Medical Devices
- Wearable/Mobile Electronics
- Powered Exoskeleton suits

What is electromyography?

Measuring muscle activation via electric potential, referred to as electromyography (EMG), has traditionally been used for medical research and diagnosis of neuromuscular disorders. However, with the advent of ever shrinking yet more powerful microcontrollers and integrated circuits, EMG circuits and sensors have found their way into prosthetics, robotics and other control systems.

PIN LAYOUT

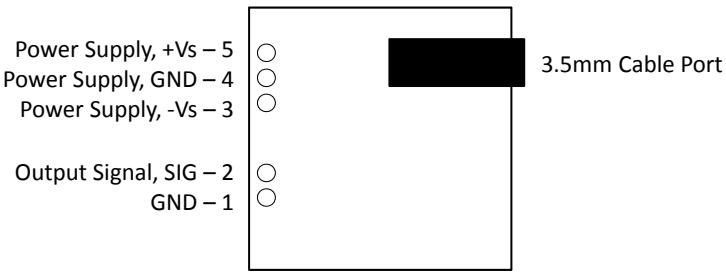

 www.AdvancerTechnologies.com AdvancerTechnologies@gmail.com

Getting Started Using Two 9V Batteries

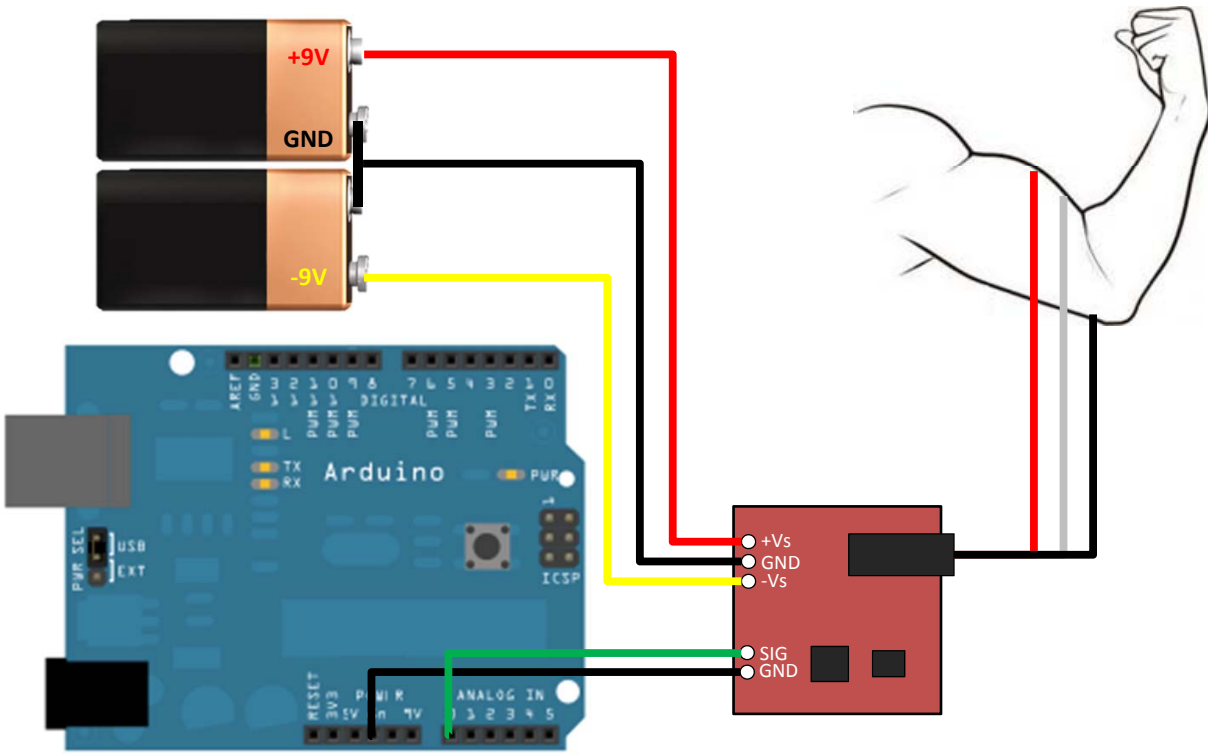

1) Connect the power supply (two 9V batteries)
   a. Connect the positive terminal of the first 9V battery to the +Vs pin on your sensor.
   b. Connect the negative terminal of the first 9V battery to the positive terminal of the second 9V battery. Then connect to the GND pin on your sensor.
   c. Connect the negative terminal of the second 9V battery to the –Vs pin of your sensor.
2) Connect the electrodes
   a. After determining which muscle group you want to target (e.g. bicep, forearm, calf), clean the skin thoroughly.
   b. Place one electrode in the middle of the muscle body, connect this electrode to the RED Cable's snap connector.
   c. Place a second electrode at one end of the muscle body, connect this electrode to the Blue Cable's snap connector.
   d. Place a third electrode on a bony or non-muscular part of your body near the targeted muscle, connect this electrode to the Black Cable's snap connector.
3) Connect to a Microcontroller (e.g. Arduino)
   a. Connect the SIG pin of your sensor to an analog pin on the Arduino (e.g. A0)
   b. Connect the GND pin of your sensor to a GND pin on the Arduino.

Dimensions

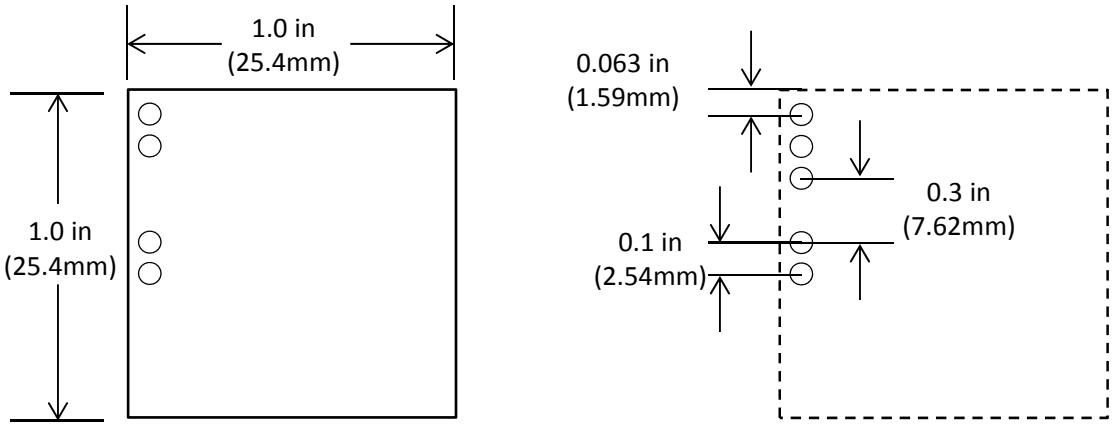

Circuit Schematic

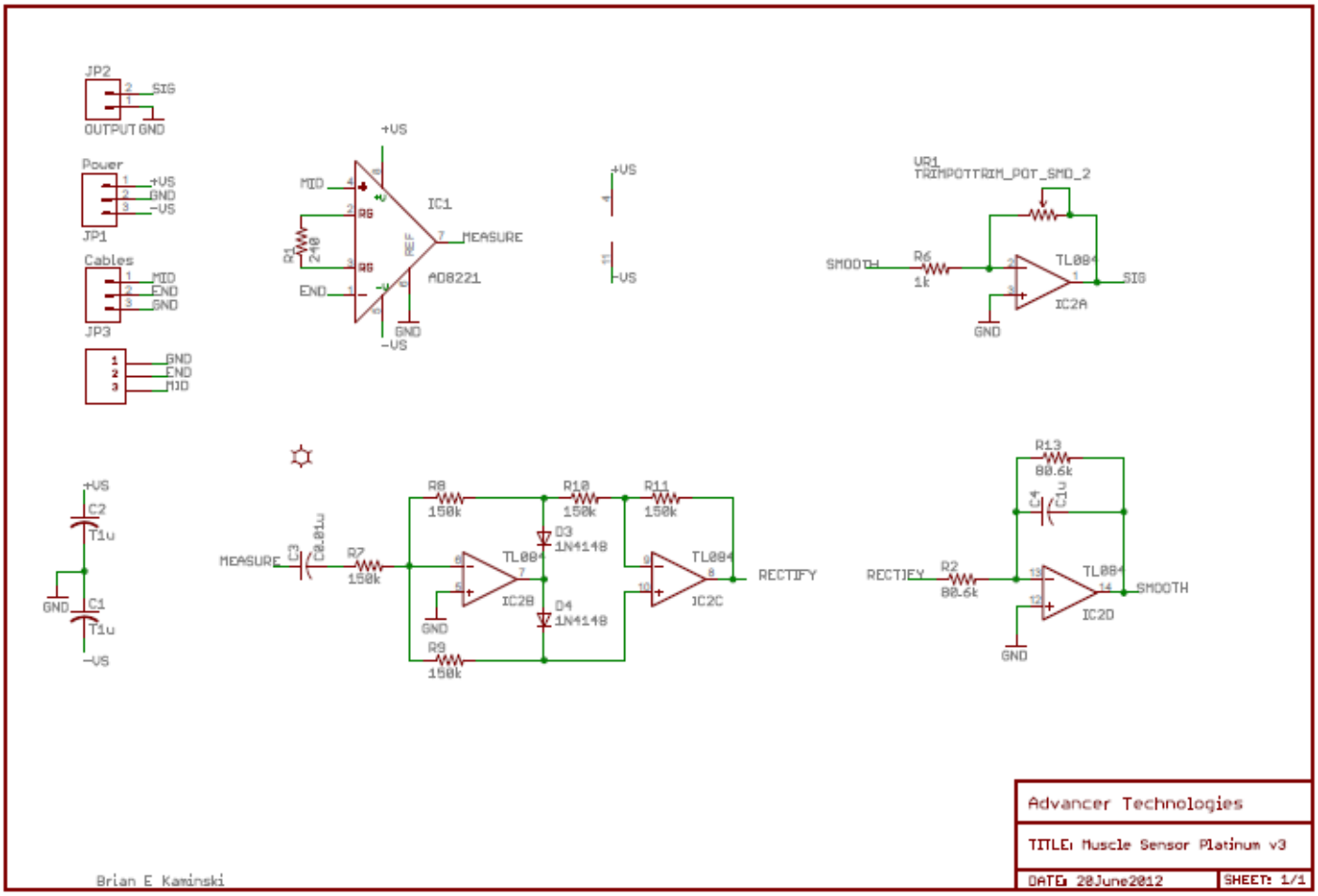

Electrical Specifications

Parameter	Min	TYP	Max
Power Supply Voltage (Vs)	±3V	±5V	±30V
Gain Setting, Gain = 207*(X /1 kΩ)	0.01 Ω (0.002x)	50 kΩ (10,350x)	100 kΩ (20,700x)
Output Signal Voltage (Rectified & Smoothed)	0V	--	+Vs
Differential Input Voltage	0 mV	2-5mV	+Vs/Gain

ELECTROSTATIC DISCHARGE SENSITIVITY

This sensor can be damaged by ESD. Advancer Technologies recommends that all sensors be handled with appropriate precautions. Failure to observe proper handling and installation procedures can cause damage.

ESD damage can range from subtle performance degradation to complete device failure.

RAW EMG vs Rectified & Smoothed EMG

Our Muscle Sensors are designed to be used directly with a microcontroller. Therefore, our sensors do not output a RAW EMG signal but rather an amplified, rectified, and smoothed signal that will work well with a microcontroller's analog-to-digital converter (ADC). This difference can be illustrated by using a simple sine wave as an example.

RAW Sine Wave

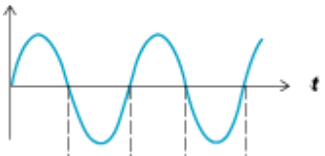

Full Wave Rectified Sine Wave

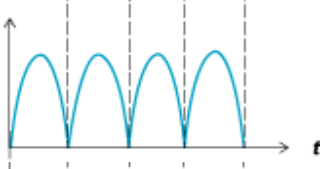

Rectified & Smoothed Sine Wave

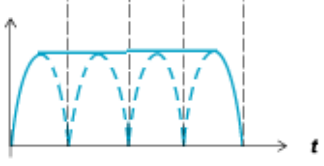

A.3. Ethics Committee Report

COMILLAS
UNIVERSIDAD PONTIFICIA
ICAI ICADE CIHS

Madrid, 18 de abril de 2023

Dictamen 38/22-23

Para: Excmo. Vicerrector de Investigación y Profesorado

Asunto: Juicio del Comité de Ética acerca del Trabajo de Fin de Grado titulado: "PREPROCESSING OF EMG SIGNALS", presentado por el alumno de la Escuela Superior de Ingeniería, D. Álvaro Martín Martín.

El Comité de Ética de la Investigación de la Universidad Pontificia Comillas, conforme al procedimiento establecido, siendo valorado el caso por sus miembros y a propuesta de su representante de la Escuela Superior de Ingeniería, emite el siguiente DICTAMEN:

Este proyecto vela por salvaguardar la dignidad de los participantes en el mismo. Es un proyecto bien estructurado y su metodología es adecuada. En él se estudia el preprocesamiento de señales electromiográficas (EMG) para control de prótesis motorizadas. Los riesgos de los participantes son mínimos pues los aparatos que se utilizan en la investigación son seguros para su uso en laboratorios de electrónica. Los participantes en el proyecto son expertos en el ámbito sanitario que obtienen información para mejorar el diagnóstico y el tratamiento de personas con discapacidad parcial. La investigación no se lleva a cabo ni con menores ni con grupos vulnerables. Por tanto, el trabajo de investigación es conforme con los principios de la Declaración de Helsinki, en cuanto resultan mayores sus beneficios que sus riesgos.

Los participantes en el proyecto gozan de autonomía para determinar si intervienen o no en el mismo, siendo también informados de que en cualquier momento pueden retirar su consentimiento para participar sin necesidad de dar explicaciones. El investigador se compromete a guardar confidencialidad y anonimicidad en la recogida de datos del estudio, de forma que la identificación de los participantes no sea posible. La investigación es, pues, conforme a la Ley 3/2018 de Protección de Datos Personales y demás legislación concordante.

El proyecto merece un juicio de conformidad ética para una investigación de sus características, y cuenta con la aprobación de este Comité.

Atentamente,

Dr. Miguel Grande Yáñez
Presidente

Dr. Raúl González Fabre
Secretario

UNIVERSIDAD PONTIFICIA COMILLAS
Alberto Aguilera, 23. 28015 Madrid. Tel.: (+34) 91 542 28 00 www.comillas.edu

Bibliography

[1] E. Criswell, *Cram's introduction to Surface Electromyography*, 2nd ed., E. ELEANOR CRISWELL, Ed. Massachussetts: JONES and BARTLETT PUBLISHERS, 1998.

[2] J. G. Webster, *Medical Instrumentation: Application and Design*. John Wiley & Sons, 1998.

[3] M. C. Staff. «Electromyography (emg)». (2023), [Online]. Available: https://www.mayoclinic.org/tests-procedures/emg/about/pac-20393913?p=1.

[4] NHONKOHDEN. «Neuropackx1». (2023), [Online]. Available: https://eu.nihonkohden.com/es/products/neurology/neuropack_x1.html.

[5] H. Tankisi *et al.*, «Standards of instrumentation of emg», *Clinical Neurophysiology*, vol. 131, no. 1, pp. 243–258, 2020. [Online]. Available: https://www.sciencedirect.com/science/article/pii/S1388245719311782.

[6] Pololu. «Advancer technologies muscle sensor v3». (2023), [Online]. Available: https://www.pololu.com/product/2726.

[7] X. Navarro, T. B. Krueger, N. Lago, S. Micera, T. Stieglitz, and P. Dario, «A critical review ofinterfaces with the peripheral nervous system for the control of neuroprostheses and hybridbionic systems.», *Journal of the Peripheral Nervous System*, 2005.

[8] V. M. Bernard Grundlehner. «Encyclopedia of biomedical engineering». (2019), [Online]. Available: https://www.sciencedirect.com/topics/engineering/motion-artifact#:~:text=Motion%20artifacts:%20Motion%20artifacts%20occur,contact%20pressure%20to%20the%20skin..

[9] H. Tam and J. G. Webster, «Minimizing electrode motion artifact by skin abrasion», *IEEE Transactions on Biomedical Engineering*, vol. BME-24, no. 2, pp. 134–139, 1977.

[10] B. B. Murphy, «Time evolution of the skin electrode interface impedanceunder different skin treatments», 2021.

[11] R. H. Chowdhury, M. B. I. Reaz, M. A. B. M. Ali, A. A. A. Bakar, K. Chellappan, and T. G. Chang, «Surface electromyography signal processing and classification techniques», *Sensors*, vol. 13, no. 9, pp. 12 431–12 466, [Online]. Available: https://www.mdpi.com/1424-8220/13/9/12431.

[12] R. A. Mezzarane and A. F. Kohn, «A method to estimate emg crosstalk between two muscles based on the silent period following an h-reflex», *Medical Engineering & Physics*, vol. 31, no. 10, pp. 1331–1336, 2009. [Online]. Available: https://www.sciencedirect.com/science/article/pii/S1350453309002057.

[13] . D. B. H. R. Plonsey, *Considerations of quasi-stationarity in electrophysiological systems*. 1967, pp. 657–664.

[14] N. S. Stoykov, M. M. Lowery, A. Taflove, and T. A. Kuiken, «A finite element analysis of muscletissue capacitive effects and dispersion in emg», 2001.

[15] E. M. Purcell and D. J. Morin, *Electricity and Magnetism (Third Edition)*. Cambridge University Press, 2013, 853 pp.

[16] M. A. Hemingway, H. J. Biedermann, and J. Inglis, «Electromyographic recordings of paraspinalmuscles: Variations related to subcutaneous tissue thickness», *Biofeedback Selfregul*, 1995.

[17] S. Lobov, N. Krilova, I. Kastalskiy, V. Kazantsev, and V. A. Makarov, *Emg data for gestures data set*, UCI, Ed., 2019. [Online]. Available: https://archive.ics.uci.edu/ml/datasets/EMG+data+for+gestures#.

[18] M. Paligaru. «Review: The future is now with the myo gesture control armband». (2015), [Online]. Available: https://blog.bestbuy.ca/wp-content/uploads/2015/12/36200i07F8DD5290DCC798.jpg.

[19] AnalogDevices. «Ad8422 datasheet». (2023), [Online]. Available: https://www.alldatasheet.com/datasheet-pdf/pdf/504093/AD/AD8422.html.

[20] H. Zumbahlen. «Linear circuit design handbook». (2008), [Online]. Available: https://www.analog.com/en/education/education-library/linear-circuit-design-handbook.html.

[21] R. F. Coughlin and F. F.Driscoll, *Operational Amplifiers and Linear Integrated Circuits (6th Ed.)* Prentice Hall, 2001.

[22] AnalogDevices. «Envelope detector». (2021), [Online]. Available: https://wiki.analog.com/university/courses/electronics/electronics-lab-envelope-detector.

[23] R. Keim. «When a diode simply isn't good enough: The superdiode». (2018), [Online]. Available: https://www.allaboutcircuits.com/technical-articles/when-a-diode-simply-isnt-good-enough-the-superdiode/.

[24] C. S. Bretherton. «Lecture 11: White and red noise». (2014), [Online]. Available: https://atmos.washington.edu/~breth/classes/AM582/lect/lect8-notes.pdf.

[25] A. Phinyomark, F. Quaine, S. Charbonnier, C. Serviere, F. Tarpin-Bernard, and Y. Laurillau, «Feature extraction of the first difference of emg time series for emg pattern recognition», *Computer Methods and Programs in Biomedicine*, vol. 117, no. 2, pp. 247–256, 2014. [Online]. Available: https://www.sciencedirect.com/science/article/pii/S0169260714002478.

[26] X. Hu, Z. Wang, and X. Ren, «Classification of surface emg signal using relative wavelet packet energy», *Computer Methods and Programs in Biomedicine*, vol. 79, no. 3, pp. 189–195, 2005. [Online]. Available: https://www.sciencedirect.com/science/article/pii/S0169260705000854.

[27] NIH. «Anatomy, shoulder and upper limb, forearm flexor carpi ulnaris muscle». (2023), [Online]. Available: https://www.ncbi.nlm.nih.gov/books/NBK526051/#:~:text=Flexor%20carpi%20ulnaris%20is%20a,connected%20by%20a%20tendinous%20arch..

[28] ORIMtec. «Flexor carpi ulnaris». (2011), [Online]. Available: https://www.orimtec.com/illustrations/pop-recording-sites.php?id=16.

[29] M. S. H. M.B.I. Raez and F. Mohd-Yasin, «Techniques of emg signal analysis: Detection, processing, classification and applications», *PMC*, 2006.

[30] MATLAB. «Movvar». (2023), [Online]. Available: https://es.mathworks.com/help/matlab/ref/movvar.html.

[31] MATLAB. «Movmean». (2023), [Online]. Available: https://es.mathworks.com/help/matlab/ref/movmean.html.

[32] B10NUMB3R5. «Reaction time - human homo sapiens». HARVARD, Ed. (2023), [Online]. Available: https://bionumbers.hms.harvard.edu/bionumber.aspx?s=n&v=2id=110799.

[33] UnitedNations. «The 17 goals». (2023), [Online]. Available: https://sdgs.un.org/goals.

[34] UnitedNations. «Ensure healthy lives and promote well-being for all at all ages». (2023), [Online]. Available: https://sdgs.un.org/goals/goal3.

[35] UnitedNations. «Build resilient infrastructure, promote inclusive and sustainable industrialization and foster innovation». (2023), [Online]. Available: https://sdgs.un.org/goals/goal9.